THE USE OF NUCLEAR MAGNETIC RESONANCE IN INORGANIC CHEMISTRY

E. L. Muetterties and W. D. Phillips

Central Research Department, Experimental Station, E. I. DuPont de Nemours, Wilmington, Delaware

I. Introduction

First experimental observations of the nuclear magnetic resonance (NMR) phenomenon were made in 1946 independently by groups working under Bloch (*7*) at Stanford and Purcell (*112*) at Harvard. For this discovery, these two physicists jointly were awarded the Nobel prize in physics in 1952. The experimental and theoretical aspects of nuclear magnetic resonance (NMR) have been developed rapidly so that today it is an indispensable technique for the investigation of a wide variety of chemical and physical phenomena.

Briefly, the physical basis of NMR is as follows. A nucleus possessing a spin quantum number $\mathbf{I}$ other than zero is endowed also with spin angular momentum, $\mathbf{p}$, given by

$$\mathbf{p} = \hbar\mathbf{I} \tag{1}$$

and a magnetic moment $\boldsymbol{\mu}$, which, when expressed as a vector quantity, is given by

$$\boldsymbol{\mu} = \gamma\hbar\mathbf{I} \tag{2}$$

and as a scalar quantity, by

$$|\mu| = \gamma\hbar\sqrt{I(I+1)}. \tag{3}$$

The magnetogyric ratio γ is a constant for a given nucleus. When a nucleus is subjected to a magnetic field $\mathbf{H}_0$, the energy of the nuclear spin system is

$$W = -\boldsymbol{\mu}\cdot\mathbf{H}_0 = -\gamma\hbar m H_0, \tag{4}$$

where m is the component of $\mathbf{I}$ along $\mathbf{H}_0$ and takes the values I, $I-1$, $I-2$, . . . , $-I$. Since the selection rule for transitions between nuclear spin states is $\Delta m = \pm 1$, we have

$$\Delta W = h\nu = \hbar\omega = \gamma\hbar H_0 \tag{5}$$

or

$$\omega = \gamma H_0, \tag{6}$$

the familiar Larmor frequency relationship. Thus we see that each nucleus that possesses a magnetic moment should exhibit a characteristic nuclear magnetic resonance absorption. Isotopic species of a given element possess different magnetogyric ratios. Empirically it is found that nuclei which contain an odd number of neutrons, an odd number of protons, or both, possess nonzero nuclear magnetic moments and consequently exhibit nuclear magnetic resonance absorption. All three isotopes of hydrogen therefore exhibit NMR absorption and, for example, whereas the O^{16} nucleus with eight protons and eight neutrons has a zero nuclear moment, the O^{17} nucleus with nine neutrons has a moment and is active in NMR absorption.

Another important nuclear characteristic is the nuclear quadrupole moment which, possessed by nuclei for which $I \geqslant 1$, has given rise to the important field of nuclear quadrupole resonance spectroscopy. A major importance of the quadrupole moment with respect to NMR absorption resides in the effects of quadrupole coupling constants on nuclear relaxation times and, therefore, on the line widths and saturation characteristics of NMR absorption (*9*). In addition, in favorable situations, quadrupole coupling constants can be derived from the characteristics of nuclear resonance of quadrupolar nuclei (*127*). Some examples of these effects will be described in Sections III, IV and VI of this chapter.

From the above brief discussion it is difficult to imagine how NMR could have had the revolutionary impact on our understanding of the electronic and geometrical structures of molecules that it has had. However, in the period 1949–51, spectrometer systems (particularly magnets) were refined to the point where chemical shifts and nuclear spin-spin splittings became resolvable. It is, of course, from these two rather small effects (small energy-wise) that NMR derives its primary usefulness to chemistry.

In the discussion to follow certain aspects of chemical shifts and nuclear spin-spin interactions will be reviewed. However, it is not our intention to give the theories of these effects with any degree of completeness since excellent treatments may be found in reviews and the original literature (*108*). We only hope here to point out some results and approaches of NMR particularly applicable to inorganic systems. Let it suffice at this point to say that chemical shifts of nuclei arise from shielding effects of nearby electrons. The field H_{eff} "seen" by the nucleus is not the externally applied field H_0, but

$$H_{\text{eff}} = H_0(1 - \sigma) \tag{7}$$

so that resonance for a given nucleus occurs at

$$\omega_i = \gamma_i H_0(1 - \sigma_i). \tag{8}$$

σ_i is the shielding constant for nucleus i and experimentally is defined as

$$\delta_i = \sigma_i - \sigma_{\text{ref}} = \frac{H_i - H_{\text{ref}}}{H_{\text{ref}}} \times 10^6 \tag{9}$$

H_{ref} and σ_{ref} refer to an arbitrarily chosen reference. The quantities δ and σ are dimensionless and expressed in ppm.

The spin Hamiltonian for a two spin system is

$$\mathcal{H} = -\gamma_i \hbar m_i H_0(1 - \sigma_i) - \gamma_j \hbar m_j H_0(1 - \sigma_j) + A_{ij} h \mathbf{I}_i \cdot \mathbf{I}_j \tag{10}$$

The first two terms describe the chemical shifts for nuclei i and j and the last, the nuclear spin-spin interaction. Nuclear spins are coupled via intervening electrons. The coupling constant A, sometimes represented by J in the literature, is expressed in cycles per second (cps). Analyses of observed spectra for δ_i, δ_j and A_{ij} are quite straightforward in situations where $\nu_0|\delta_i - \delta_j| \gg A_{ij}$ but can become quite tedious where $\nu_0|\delta_i - \delta_j|$ and A_{ij} are comparable. ν_0 is the resonance frequency expressed in cps. The latter case is the so-called intermediate coupling situation and is discussed in detail by Pople *et al.* (*108*).

II. Chemical Shifts and Nuclear Spin-Spin Coupling Constants

A. Introduction

The two observables of nuclear magnetic resonance spectroscopy of primary interest to the chemist in the elucidation of the electronic and geometrical structures of molecules are the chemical shifts of nuclei and nuclear spin-spin coupling constants. These two parameters can be and have been used with great success in purely empirical fashion for determining the structures of molecules. A few examples illustrating the power of NMR in molecular structure determination will be given in a later section. Additionally, however, we have in chemical shifts and spin-spin coupling constants two observables which can be measured to a high degree of accuracy and which in principle reflect rather sensitively environments of individual atoms and properties of bonds in molecules. It is one of the chief tasks of theoreticians today to translate as quantitatively as possible chemical shifts and coupling constants into such molecular quantities as charge distributions, bonding hybrids and bond angles and lengths.

Quantitative theories for the chemical shift and nuclear spin-spin interaction were developed by Ramsey (*113*) soon after the experimental discoveries of the effects. Unfortunately the complete treatments of these effects involve rather detailed knowledge of the electronic structures of molecules and require evaluation of matrix elements of the orbital angular momentum between ground and excited electronic states. These matrix elements depend sensitively on the behavior of the wave function near

the nucleus, a circumstance which makes most approximate wave functions commonly used for calculations on molecules quite inadequate for evaluating chemical shifts and coupling constants from Ramsey's complete expressions.

As was to be expected, a good deal of effort has been expended in attempts to develop approximate theoretical schemes for treating chemical shifts and coupling constants. Such treatments have been of a largely semiempirical nature and often have been based on observed experimental regularities. Resonances of a large number of nuclei can be observed experimentally, and many of these have been studied with varying degrees of thoroughness. However, properties such as hybridization, ionic characters of bonds, electron density, low-lying electronic states, and magnetic anisotropies of nearby atoms or groups dominate the NMR observables of different nuclei to varying extents. For this reason, no one semiempirical or approximate treatment should be expected to be applicable to a very wide variety of nuclei.

B. Chemical Shifts

Most experimental studies to date have been carried out on the H^1 nucleus in organic molecules and for this reason understanding of the NMR characteristics of hydrogen is most advanced. Contributions to proton chemical shifts include diamagnetic shieldings (electron density effects) (*21*, *24*, *32*), ring currents (*56*, *107*, *136*) electrostatic field effects (*10*, *33*, *82*) and magnetic anisotropies of atoms and bonds in molecules (*11*, *72*). Chemical shifts for protons and most other nuclei also are sensitive to intermolecular environmental influences such as solvent-solute interactions. Further discussion of proton shifts will be deferred to later sections where specific effects arising in hydrides, organometallics and paramagnetic chelates are reviewed. A few examples of chemical shifts in more typically inorganic nuclei will be discussed in the remainder of this section where it appears that some theoretical significance can be attached to observed chemical shifts.

Chemical shifts, as treated by Ramsey (*113*), are comprised of separate diamagnetic and paramagnetic contributions. The diamagnetic term was considered to arise from the response of the extranuclear electrons to the external magnetic field and had been given earlier by Lamb (*65*) as

$$\sigma_d = \frac{4\pi e^2}{3mc^2} \int_0^\infty r\rho(r)dr, \tag{11}$$

where $\rho(r)$ is the electron density at a distance r from the nucleus. Reasonably good estimates of this term for many atoms could be made from existing Hartree functions. However, the paramagnetic term in its complete form

proved difficult to handle, principally because of inadequacies in existing wave functions. Saika and Slichter in an important paper in 1956 (*122*) suggested that the principal contribution to paramagnetic shielding in atoms such as fluorine arose from local magnetic fields set up by orbital motions of the electrons of $2p$ orbitals as a result of unequal electron populations of the $2p_x$, $2p_y$, and $2p_z$ orbitals. This term is given by the expression

$$\sigma_p = -\frac{2e^2h^2}{3m^2c^2}\left\langle\frac{1}{r^3}\right\rangle_{av}\frac{1}{\Delta E}. \tag{12}$$

Here $\langle 1/r^3\rangle_{av}$ is the average value of $1/r^3$ for a $2p$-orbital and ΔE is an "average" electronic excitation energy. This expression goes to zero for F^- where $N_x = N_y = N_z$. N_x, N_y, and N_z are respectively the numbers of electrons occupying the $2p_x$, $2p_y$, and $2p_z$ orbitals.

The treatment of Saika and Slichter has served as model for several subsequent calculations of chemical shifts of nuclei other than hydrogen. The most successful of these calculations have been those of Griffith and Orgel (*39*) and Freeman *et al.* (*35*) on the shifts of complexed Co^{59}(III). Shifts for Co^{59}(III) in a variety of octahedrally coordinated complexes are shown in Table I. The range of 14,000 ppm in chemical shifts for these rather similarly constituted complexes is such as to suggest that a para-

TABLE I

Co^{59} SHIFTS IN SOME OCTAHEDRALLY COORDINATED COBALT COMPLEXES (*35*)

Compound	Cobalt resonance frequency (Mc/sec) at 4370.9 gauss	Positions of absorption maxima (mμ)	
Potassium hexacyanocobaltate(III)	4.4171	311	259
Lithium tetranitrodiamminecobaltate(III)	4.4478	426	347
Trans-dichlorobis(ethylenediamine)cobalt(III) chloride	4.4485	505	—
Carbonatobis(ethylenediamine)cobalt(III) bromide	4.4486	512	358
Tris(ethylenediamine)cobalt(III) chloride	4.4488	470	340
Trans-dinitrotetramminecobalt(III) chloride	4.4489	445	—
Tris(propylenediamine)cobalt(III) chloride	4.4490	470	340
Cis-dinitrotetramminecobalt(III) chloride	4.4493	450	—
Sodium hexanitrocobaltate (III)	4.4502 (strong) 4.4527 (weak)	480	358
Hexamminecobalt(III) chloride	4.4534	475	338
Carbonatotetramminecobalt(III) nitrate	4.4575 4.4601	512	—
Cobalt(III) trisacetylacetonate (in benzene)	4.4731	597	—
Potassium trioxalatocobaltate(III)	4.4747	610	425
Tricarbonatocobalt(III) nitrate	4.4795	645	444

magnetic contribution completely swamps any effects of diamagnetic shielding.

Assuming the strong field approximation, the ground state of Co(III) in octahedral complexes has the configuration $(t_{2g})^6$ and is of $^1A_{1g}$ symmetry. Nonvanishing matrix elements of the orbital angular momentum exist between the $^1A_{1g}$ ground state and the excited state of configuration $(t_{2g})^5(e_g)^1$ and symmetry $^1T_{1g}$. The calculation then gives the result that the chemical shift σ for Co(III) should be of the form

$$\sigma = A - \frac{B}{\Delta E} \tag{13}$$

where A is the Lamb diamagnetic shielding, B is proportional to the matrix element of the orbital angular momentum between the states $^1A_{1g}$ and $^1T_{1g}$, and ΔE is the energy separation between the $^1A_{1g}$ ground state and the singly excited ^1T_1g state. ΔE is approximately the crystal field splitting of cobalt by the ligands. Values of ΔE were obtained from spectral studies. A plot of ΔE vs. σ (Fig. 1) for a series of Co(III) complexes is fairly linear,

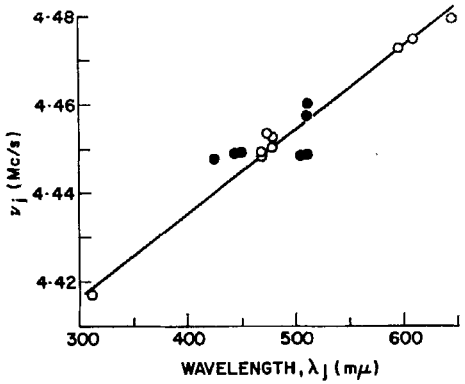

FIG. 1. Co^{59} chemical shifts vs. ΔE_{dd} for some octahedrally coordinated Co(III) complexes. [Freeman *et al.* (*34*).]

confirming the general validity of the treatment. Values of σ obtained using Eq. (13) and calculated values of A and B give rather good agreement with experimental determinations of Co(III) shifts. Finally, chemical shifts for Co(III) in these complexes exhibit wide temperature variations (*35*, *39*). These variations were attributed to the temperature dependence of the crystal field splitting, caused in turn by thermal excitation of higher vibrational modes of the complex. This prediction of the model also is borne out rather well experimentally.

This analysis of the chemical shifts of octahedrally coordinated Co(III) in terms of ligand field effects should point the way to many future studies

of metal resonances of diamagnetic organometallics and transition metal chelates. It should be noted that the success of the above treatment depended on the fact that one of the several possible contributing mechanisms to the nuclear shielding of cobalt dominates. As we shall see later, a similar favorable circumstance is encountered with the contact interaction shifts of certain paramagnetic transition metal chelates. Another situation favorable at least in principle is encountered with covalently bound chlorine where not only is one mechanism expected to dominate chemical shifts but the shifts are expected to be related to another measurable quantity, namely, the quadrupole coupling constant.

To a first approximation, bonding of fluorine or chlorine in a saturated system involves only the $2p_z$ orbital for fluorine and the $3p_z$ orbital for chlorine. From the treatment of F^{19} chemical shifts by Saika and Slichter (*122*), the paramagnetic contribution to the shifts can be considered as arising from charge deviations from spherical symmetry about the fluorine nucleus. Since N_x, N_y, and N_z are the numbers of electrons occupying respectively the $2p_x$, $2p_y$, and $2p_z$ orbitals, then, qualitatively, a paramagnetic contribution to the shift arises where $N_x = N_y \neq N_z$. However, in the treatment of Townes and Dailey (*131*, *132*) such deviations from spherical charge symmetry about quadrupolar nuclei are what give rise to nonzero nuclear quadrupolar coupling constants for atoms in molecules. A connection, therefore, is expected between paramagnetic contributions to nuclear shieldings and nuclear quadrupole coupling constants.

Masuda examined the relationship between Cl^{35} quadrupole coupling constants and chemical shifts in the series $SiCl_4$, $TiCl_4$, $VOCl_3$, and CrO_2Cl_2 (*83*). By the procedure of Townes and Dailey (*131*, *132*), quadrupole coupling constants e^2qQ are given by

$$e^2qQ = (1 - s)(1 - i)e^2q_0Q \tag{14}$$

where s is the s-character of the chlorine bonding hybrid, i is the ionic character of the bond, and e^2q_0Q is the quadrupole coupling constant for the chlorine atom ($N_x = N_y = 2$, $N_z = 1$). Application of the Saika and Slichter treatment (*122*) to chlorine gives for the chemical shift,

$$\sigma = \delta_{Cl} - \delta_{Cl^-} = -(1 - s)(1 - i)\frac{2}{3}\frac{e^2h^2}{m^2c^2}\left\langle\frac{1}{r^3}\right\rangle_{3p}\frac{1}{\Delta E} \tag{15}$$

where ΔE is an average excitation energy. Thus it would be predicted that σ should be proportional to e^2qQ at least for a series of molecules for which $1/\Delta E$ remains sensibly constant. That such is not the case for the above series of inorganic chlorides is seen from Fig. 2 where σ vs. e^2qQ is not linear and σ actually decreases as e^2qQ increases. Values of 1 ev, 2 ev, 3 ev, and

15 ev must be assigned to ΔE for $TiCl_4$, $VOCl_3$, CrO_2Cl_2, and $SiCl_4$ to bring observed values of σ and e^2qQ into agreement with the predictions of theory.

The theory connecting σ and e^2qQ is highly approximate and neglects among other things effects of d-orbital hybridization which may be fairly important in these molecules. Ignorance of appropriate values of $1/\Delta E$ also makes comparison between theory and experiment awkward. A more appropriate test of the relationship between σ and e^2qQ would be in a series

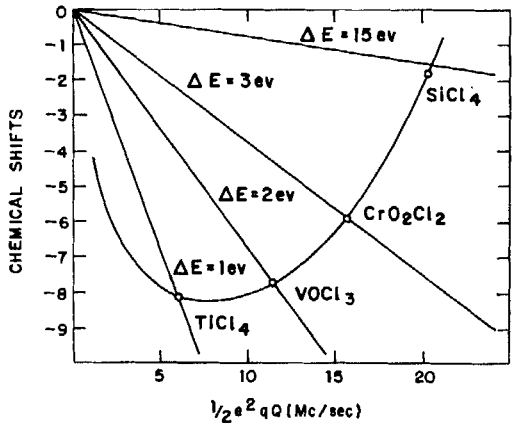

FIG. 2. Cl^{35} chemical shifts vs. Cl^{35} quadrupole coupling constants for some covalent chlorides. [Masuda (*83*).]

of molecules for which d-orbital hybridization would be expected to be small and for which $1/\Delta E$ values could be expected to be similar. Such a series is provided by the chlorinated methanes where a number of e^2qQ values are known to a high degree of accuracy. Values of σ and e^2qQ for CH_2Cl_2, $CHCl_3$, and CCl_4 are given in Table II (*101*). While a linear rela-

TABLE II

CORRELATION BETWEEN σ AND e^2qQ FOR SOME ORGANIC CHLORIDES (*101*)

Compound	σ (gauss shift from Cl^- at 10,000 gauss)	e^2qQ (Mc/sec)
CH_2Cl_2	−2.8	72.4
$CHCl_3$	−4.5	77.0
CCl_4	−7.3	81.8

tion between σ and e^2qQ is not observed, here at least σ increases with e^2qQ without variations in $1/\Delta E$ having to be invoked. More complete studies of theoretical and experimental nature will be required to establish the extent to which σ and e^2qQ can be correlated.

C. Nuclear Spin-Spin Coupling

Empirically it was found that the field independent fine structure superimposed on the chemical shifts of NMR spectroscopy could be described by an interaction energy, $E_{NN'}$, between nuclear spin vectors $\mathbf{I}_N$ and $\mathbf{I}_{N'}$ of the form (*46*, *48*)

$$E_{NN'} = hA_{NN'}\mathbf{I}_N \cdot \mathbf{I}_{N'} \tag{16}$$

where h is Planck's constant and $A_{NN'}$ is characteristic of the molecule containing nuclei N and N'. Quantum mechanically, the nuclear spin-spin interaction energy is given by

$$E_{NN'} = \frac{\int \psi \mathcal{H}_{NN'} \psi d\tau}{\int \psi \psi d\tau}, \tag{17}$$

where $\mathcal{H}_{NN'}$ is the Hamiltonian describing the interaction between N and N'. There are several possible contributions to $\mathcal{H}_{NN'}$ (*114*, *115*) but it appears that in most cases the Fermi interaction (*29*) is the dominant one. The Fermi or contact interaction takes the form

$$\mathcal{H}_{\text{contact}} = \frac{16\pi\beta h}{3} \sum_k \sum_N \gamma_N \delta(r_{kN}) \mathbf{S}_k \cdot \mathbf{I}_N \tag{18}$$

where the k's refer to electrons and the N's to nuclei. γ_N is the magnetogyric ratio of nucleus N, $\delta(r_{kN})$ is a delta function that vanishes except when there is a finite probability of electron k being located at nucleus N, and $\mathbf{S}_k$ is the electron spin vector. Perturbation theory gives the result that the contribution to $A_{NN'}$ by the contact interaction is

$$A_{NN'}^{\text{contact}} = -\frac{2}{3h} \frac{16\pi\beta h^2}{3} \frac{\gamma_N \gamma_{N'}}{\Delta E} \left| 0 \right| \sum_k \sum_j \delta(r_{kN}) \delta(r_{jN'}) S_k S_j \left| 0 \right| \tag{19}$$

where ΔE again is an average electronic excitation energy.

A calculation of the contact contributions to nuclear spin coupling in the H-D molecule has been carried out (*114*) using the James-Coolidge wave function (*55*). This calculation gave

$$A_{HD}^{\text{contact}} = \frac{55.8}{\Delta E} \text{ cps} \cong 40 \text{ cps}. \tag{20}$$

Experimentally, $A_{HD} = 44$ cps, so that considerable weight can be given the contact interaction as a primary contributor to nuclear spin-spin splittings, at least where hydrogen is involved.

Molecular wave functions of the accuracy of the James-Coolidge function do not, of course, exist except for the H_2 molecule. Consequently avail-

able molecular orbital and valence bond functions have been used for approximate calculations of $A_{NN'}^{contact}$ in more complicated molecules. For example, McConnell (*71*) has shown using a molecular orbital wave function that proton-proton couplings are given by

$$A_{HH'} \cong 200\eta_{HH'}^2 \text{ cps.} \tag{21}$$

The factor $\eta_{HH'}$ is the bond order between the interacting hydrogen atoms and is unity for H_2. Proton-proton bond orders in substituted benzenes as derived from coupling constants and Eq. (21) are given in Table III. The same quantitative significance should not be attached to the proton-proton bond orders of Table III that one gives to the carbon-carbon

TABLE III
PROTON-PROTON BOND ORDERS IN BENZENES AS DERIVED FROM COUPLING CONSTANTS

Proton pairs	$A_{HH'}$	$\eta_{HH'}$
Ortho	7.9	0.2
Meta	2.1	0.1
Para	0.5	0.05

π-bond orders often calculated for conjugated organic systems using, for example, the Hückel LCAO MO approach (*19*). The chief significance of η resides in its emphasis that spin-spin interactions between nonbonded nuclei in molecules only exist because the spins of electrons centered on the interacting nuclei are not entirely uncorrelated.

In this light Eq. (21) has been given the following statistical interpretation (*71*). Consider two hydrogen atoms N and N′ in a molecule not necessarily bonded directly. Then let

$$P(\overset{\alpha}{N}\ \overset{\beta}{N'}) \equiv P^{\alpha\beta}$$

be the probability at any instant for the 1s electrons of the two hydrogen atoms to have antiparallel spin alignment and

$$P(\overset{\alpha}{N}\ \overset{\alpha}{N'}) \equiv P^{\alpha\alpha}$$

be the probability for parallel spin alignment. Then

$$A_{NN'} \propto (P^{\alpha\beta} - P^{\alpha\alpha}). \tag{22}$$

Thus nuclear spin-spin coupling between protons N and N′ that are not directly bonded is a measure of the spin correlation between the 1s electrons of the two hydrogen atoms. This concept of spin correlation between non-

bonded protons has been used by Hecht *et al.* (*51*) to give a quantitative and convincing explanation for the barrier to internal rotation in ethanes.

Calculations of nuclear spin-spin couplings by Karplus and co-workers (*60*) using valence bond functions* have been gratifyingly successful. It was to be expected that valence bond functions would be more accurate than LCAO MO functions for this purpose since the former include explicitly effects of spin correlation. For interactions between nonbonded nuclei such as occur, for example, between the hydrogen atoms of CH_4 or NH_4^+, structures of the forms (*61*)

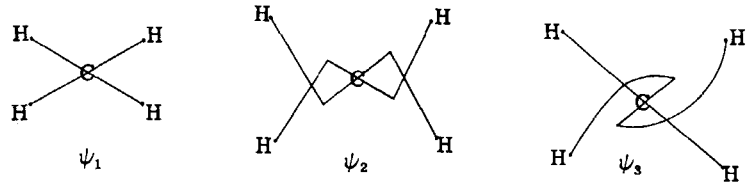

are considered to be the primary contributors to the ground state wave function. Bond structures ψ_2 and ψ_3 may be considered to represent deviations from perfect pairing. For CH_4, the ground state wave function obtained from solution of the appropriate secular equations is (*61*)

$$\psi_0 = 1.08\psi_1 + 0.001\psi_2 - 0.028\psi_3. \tag{23}$$

Use of this wave function with Eq. (19) then yields a theoretical value for A_{HH} in CH_4 of 12.5 cps which is to be compared with the experimental value of 12.3 ± 0.6 cps. Valence bond calculations of this nature have successfully accounted for the variation with H—C—H angle of the proton-proton coupling constants in substituted methanes (*45*) (Fig. 3), for the difference between $A_{HH'}^{cis}$ and $A_{HH'}^{trans}$ across double bonds in ethylenes, and for the difference between $A_{HH'}^{trans}$ and $A_{HH'}^{gauche}$ across C—C bonds in ethanes (*59*).

Nuclear spin-spin interactions between directly bonded nuclei also are considered to proceed primarily via the Fermi contact interaction mechanism. Here, however, there is no need to consider structures representing deviations from perfect pairing and indeed such have been ignored in calculations to date as of being of secondary importance.

Karplus and Grant (*61*) have considered from the LCAO MO point of

* Actually it is a defect of the simple Hückel LCAO MO approach that spin correlation is not included and is responsible for poor success of these approximate wave functions in calculating nuclear spin-spin interactions and also spin density distributions in nonalternate and odd alternate paramagnetic molecules.

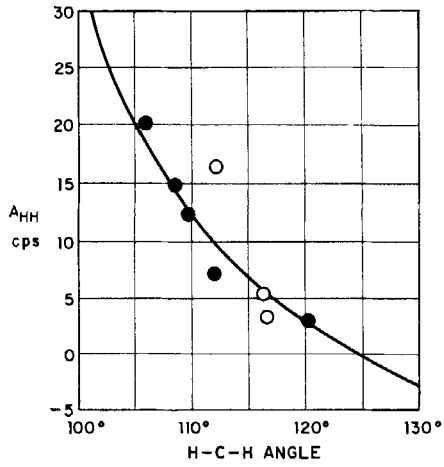

FIG. 3. A_{HH} vs. H—C—H angle in some methanes. [Gutowsky *et al.* (*45*).]

view M—H coupling constants in the series of tetrahedral molecules BH_4^-, CH_4, and NH_4^+. Tetrahedral hybrid orbitals of the form

$$\varphi = \frac{1}{2}s + \frac{3}{2}p\sigma$$

were employed for the bonding orbitals of M. Ionic terms as well as covalent were included in the wave function since contact spin-spin interactions are transmitted only if the bond has a nonvanishing covalent character. Using measured values of A_{HH}, the quantities $[\eta^2\tau^2]$ were calculated which should be related to the bond ionic characters. Comparisons between calculated and "experimental" ionic characters are given in Table IV and are seen to be in reasonably good agreement when one considers the approximations inherent in the calculation and the rather ambiguous nature of "experimental" ionic characters.

TABLE IV

COMPARISON BETWEEN IONIC CHARACTERS OF BONDS DERIVED FROM EXPERIMENT AND CALCULATED FROM COUPLING CONSTANTS (*61*)

Species	A_{MH} (cps)	X_M-X_H	$[\eta^2\tau^2]$
BH_4^-	80.5	0.07	0.02
CH_4	124	0.14	0.047
NH_4^+	53.5	0.27	0.096

M—H ionic characters calculated by the above procedure then were employed (*61*) to compute A_{MH} coupling constants for the nontetrahedral

series of molecules B_2H_6, C_2H_4, and NH_3. Orbitals centered on M were taken to be of the form

$$\varphi = as + bp\sigma;$$

a and b were adjusted for each of the three molecules to give hybrid orbitals having directional properties consistent with the known bond angles. Comparisons between calculated and experimental values of A_{MH} for these three molecules are shown in Table V. Agreement between theory and experiment is quite good here and suggests further fruitful applications of this approach.

TABLE V
CALCULATED AND EXPERIMENTAL COUPLING CONSTANTS (*61*)

Molecule	H—M—H angle	a^2	A_{MH} (cps) (calculated)	A_{MH} (cps) (experimental)
B_2H_6	121.5°	0.337	109	125 ± 2
C_2H_4	117.4°	0.315	156	157 ± 2
NH_3	106.8°	0.224	48	46 ± 2

Muller and Pritchard (*90*) have considered the effects of orbital hybridization of carbon on $A_{C^{13}H}$ for C—H bonds. They used a C—H bond orbital of the form

$$\psi = a(1s_H) + b(2s_C) + c(2p\sigma), \tag{24}$$

where $a^2 + b^2 + c^2 = 1$, and $a^2 = \frac{1}{2}$ for a nonpolar bond. The important term in $A_{C^{13}H}$ using this function was found to be

$$A_{C^{13}H} = A_0 a^2 b^2, \tag{25}$$

where A_0 is a constant characteristic of a C—H bond (independent of carbon orbital hybridization) and is to be determined empirically. Comparison between experimental and theoretical values of A_{CH} for a series of hydrocarbons is shown in Table VI. A_{CH} of 125 cps for CH_4 was used to determine A_0. Agreement between theory and experiment for sp^2 and sp carbon orbital hybridization is seen to be remarkably good.

A qualitatively similar dependence of A_{BH} on boron orbital hybridization is noted in boron hydrides (*104*). $A_{BH} = 81$ cps for BH_4^- where boron is tetrahedral while $A_{BH} = 136$ cps for borazole where boron presumably is sp^2. A_{BH} for BH_3 adducts with ethers, amines, and phosphines range between 90 and 103 cps and for these compounds boron quadrupole coupling constants have been interpreted (*22*) in terms of a boron hybridization intermediate between sp^2 and sp^3. However, the simple dependence of

A_{CH} on carbon orbital hybridization in hydrocarbons is not found to hold quantitatively for the boron hydrides.

The principal M—F coupling mechanism in inorganic fluorides also is believed to be via the Fermi contact interaction. Here, even semiquantitative treatment is much more difficult. M—F coupling is possible through

TABLE VI
SOME COUPLING CONSTANTS BETWEEN DIRECTLY BONDED H AND C^{13} (*90*)

Molecule	A_{CH} (cps) (experimental)	A_{CH} (cps) (theoretical)
Cyclohexane	123	(125)
CH_4	125	
$(CH_3)_4C$	124	
$CH_3—C\equiv C—CH_3$	131	
Ethylene	157	167
Benzene	159	
Cyclopropane	161	
$CH_3—C\equiv C^{13}—H$	248	250
$C_6H_5—C\equiv C^{13}—H$	251	

the σ-bond system only if the orbital of fluorine involved in σ-bonding contains some s-character. Also, possible M—F π-bonding must be considered. Table VII lists some P—F and Si—F coupling constants (*89*). Qualitatively it is seen here that as the s-character of the σ-bonding hybrid of P and Si is reduced, so too is A_{P-F} and A_{Si-F}.

TABLE VII
SOME P—F AND Si—F COUPLING CONSTANTS (*89*)

Compound	P or Si Bonding hybrid	A_{P-F} (cps)	A_{SiF} (cps)
PF_3	sp^3	1441	—
PF_5	dsp^3	916	—
PF_6^-	d^2sp^3	710	—
SiF_4	sp^3	—	178
$SiF_6^=$	d^2sp^3	—	110

F—F and M—F coupling constants for a series of octahedrally coordinated atoms are listed in Table VIII. BrF_5 and IF_5 may be considered to be octahedrally coordinated since a pair of nonbonding electrons occupies an axial site on the coordination sphere. F—F coupling interactions are between fluorine atoms on approximately axial and equatorial sites. In column four of Table VIII, M—F coupling constants have been divided

through by the ratio γ_M/γ_F in order to permit comparisons of magnitudes of M—F coupling constants. Little can be said at this point concerning relationships between M—F and F—F coupling constants and such properties as bond angles, bond distances, and ionic characters of bonds. Quantitative treatments of spin-spin coupling involving fluorine have yet to be made. However, the variations in F—F coupling constants are seen to be rather small over the series when one considers the variability of H—C—H coupling constants. For the few examples of Table VIII for which com-

TABLE VIII
F—F AND M—F COUPLING CONSTANTS
IN OCTAHEDRALLY COORDINATED FLUORIDES[a]

Molecules	A_{FF} (cps)	A_{MF} (cps)	$A_{MF}/\gamma_M/\gamma_F$	Reference
$(PF_5 \cdot Base_1)^\circ$	55	740	1720	(*88a*)
PF_6^-	—	710	1670	(*89*)
$(AsF_5 \cdot Base_2)^\circ$	125	995	5530	(*88*)
AsF_6^-	—	930	5170	(*89*)
$(SbF_5 \cdot Base_1)^\circ$	100	—	—	(*88*)
SbF_6^-	—	1843	7350	(*23a*)
$(WF_5 \cdot Base_1)^+$	53	72	1670	(*88*)
WF_6°	—	48	1110	(*89*)
$:BrF_5^\circ$	110	—	—	(*47, 89*)
$:IF_5^\circ$	91	—	—	(*47, 89*)
$SF_5C_6H_5$	145	—	—	(*26b*)
$SF_5C_2F_5$	145	—	—	(*89a*)
$(GeF_4 \cdot 2\ Base_3)^\circ$	70	—	—	(*88*)
$(SnF_4 \cdot 2\ Base_3)^\circ$	50	—	—	(*87*)
$(TiF_4 \cdot 2\ Base_3)^\circ$	39	—	—	(*87*)
$SF_4(SO_3F)_2$	156	—	—	(*15*)
				
$C_2F_4OC_2F_4$	93	—	—	(*89a*)

[a] $Base_1$: Amines, amides, sulfoxides, oximes; $Base_2$: Pyridine; $Base_3$: Ethers, alcohols, sulfoxides, amides, oximes.

parison is possible, there does appear to be a rough correlation between A_{FF} and $A_{MF}/\gamma_M/\gamma_F$. It is also noteworthy how insensitive are F—F and M—F coupling constants for a given MF_5 or MF_4 fluoride to the nature of the ligand employed.

III. Stereochemistry

A. INTRODUCTION

High resolution nuclear magnetic resonance spectroscopy of molecules yields, in favorable situations, separate resonances for nuclei in nonequiva-

lent environments. Intensities of the individual resonances are proportional to the number of nuclei in each environment. Superimposed on these characteristic resonances or chemical shifts are hyperfine structures arising from nuclear spin interactions between nonequivalent nuclei. Analysis of these two effects provides, in some cases, a simple, unique answer to stereochemical problems. Sample requirements are relatively simple for best spectra in high resolution NMR. The compound should be present as a liquid, gas, or in solution so that anisotropic dipole-dipole interactions that lead to line broadening are completely or almost completely averaged by fast tumbling motions. Also, the nuclei of interest ideally should have zero or small electric quadrupole moments in order to maximize nuclear relaxation times and minimize line widths since quadrupolar interactions can provide important relaxation and line broadening mechanisms in environments of nonzero electric field gradients.

The value of NMR as a structural tool has been strikingly demonstrated in organic chemistry, but examples of structures first established by NMR are few in the field of inorganic chemistry. This may reflect in part an unsatisfactory state of the inorganic synthetic art; however, a fundamental difference resides in the characteristics of the compounds intrinsic to the two disciplines. The majority of organic compounds are tractable liquids or solids and contain hydrogen atoms, an ideal nucleus from the high resolution NMR point of view. In contrast, inorganic compounds are mainly solids of generally low tractability. Furthermore, a significant fraction of inorganic compounds are not suited to high resolution NMR because (1) no magnetic nuclei are present, (2) only magnetic nuclei with large quadruople moments are present, or (3) the compound is paramagnetic.* Thus, NMR is not a panacea for inorganic structural problems; it is complementary to the growing array within the spectroscopic arsenal. A major recommendation of NMR, particularly to the synthesis chemists, is the simplicity and speed of interpretation. Even for NMR spectra complicated by second order effects, the time required for analysis is small compared to, say, vibrational analysis, three dimensional X-ray studies or a microwave investigation. In the following sections, specific structural analyses are presented. The objective here is not a comprehensive review, but a description of the potential and also the limitations of high resolution NMR in stereochemical determinations. Accordingly, examples are largely restricted to structures first established by NMR or to those that best illustrate a particular point.

B. Fluorine Compounds

The first rigorous structural determination of SF_4 was based on an analysis of the F^{19} spectrum by Cotton *et al.* (*18*). Here two resonances of

* Under certain conditions, chemical shifts and nuclear spin-spin splittings may be observed in paramagnetic species. See p. 280.

equal intensity are observed, thus establishing the presence of two fluorine atom environments each containing the same number of nuclei. This rules out tetrahedral symmetry and suggests that the nonbonding pair of electrons in SF_4 resides largely in a directed orbital. Of all the possible trigonal bipyramid and tetragonal pyramid models

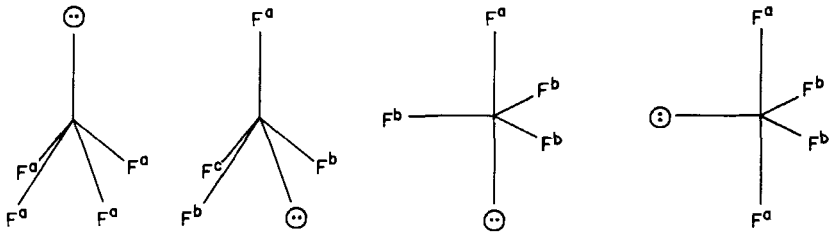

only structure (IV) the model of C_{2v} symmetry originally proposed by Dodd *et al.* (*26*), fits these data.

Superimposed on each of the SF_4 resonances is a triplet fine structure of 1:2:1 intensity ratios (Fig. 4) which reflects spin-spin coupling between nonequivalent sets of fluorine atoms. This fine structure establishes the number of nuclei per environment as two by the following line of reasoning.

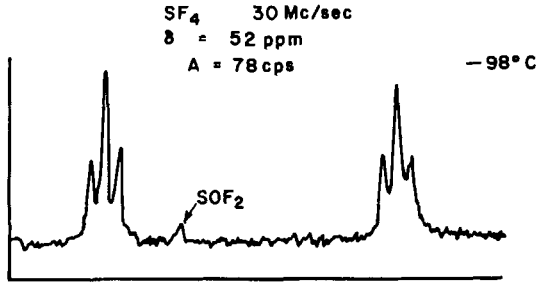

FIG. 4. F^{19} spectrum of SF_4 at −98°. [Muetterties and Phillips (*89*).]

The first-order treatment which is applicable when $\nu_0\delta \gg A$ gives the number of nuclear spin states of equivalent sets of nuclei as $2I + 1$ where I is the total spin of the equivalent set. The spin for a fluorine atom is $\frac{1}{2}$. Therefore, for the SF_4 molecule, observation of triplet fine structure establishes that $I = 1$ for an equivalent set and, consequently, that each equivalent set contains two fluorine atoms.

I	Spin states	Statistical weight
+1	$F_a\uparrow F_b\uparrow$	1
0	$F_a\downarrow F_b\uparrow$; $F_a\uparrow F_b\downarrow$	2
−1	$F_a\downarrow F_b\downarrow$	1

Such reasoning may be extended to more complicated systems. If, however, the magnitude of the spin-spin splitting is comparable to $\nu_0\delta$, the chemical shift, this first-order treatment is no longer applicable since the nuclear spin energy levels become perturbed and the spectra become more complex.* For the general analysis of NMR spectra, the reader is referred to Pople *et al.* (*109*), Roberts (*119*) and Corio (*17a*).

An excellent example of stereochemical analysis by NMR was furnished by Hoffmann *et al.* in the study of antimony pentafluoride (*53*). The F^{19} spectrum consists of three broad peaks of relative intensities 2:2:1 (Fig. 5).

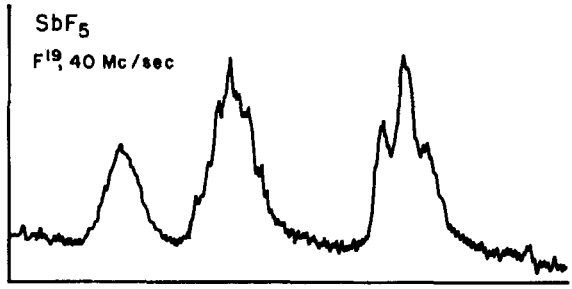

FIG. 5. F^{19} spectrum of $(SbF_5)_x$ at $\sim -10°$. Fine structure, presumably due to F-F spin coupling, is incompletely resolved. [Hoffmann *et al.* (*53*).]

No rational monomeric structure can be devised to fit these data. Actually, SbF_5 is a very viscous liquid and it must be significantly associated. Cyclic or linear polymers could be formed by association through *trans* fluorine bridge bonds. However, this type of polymer would have as the recurring unit

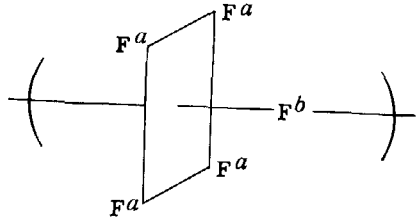

* An example may be found on p. 261.

which provides only two types of fluorine atom environments.† On the other hand, polymeric structures based on *cis*-fluorine bridge bonding do provide three distinct fluorine atom environments containing 2, 2, and 1 nuclei per SbF_5 unit. Two of the simpler possible polymers are a dimer and a cyclic tetramer.

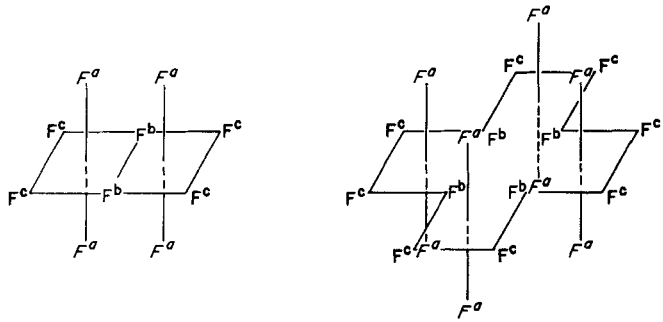

The degree of polymerization of liquid SbF_5 cannot be determined from the NMR data; the spectrum is equally consistent with dimer, cyclic trimer, tetramer, etc., and infinite chains, provided that the mode of association is *cis*-bridge bonding. This stereochemical point could probably not have been established by any other existing spectroscopic technique. A unique vibrational analysis of this complicated system seems improbable. X-ray structural analysis would be difficult because SbF_5 freezes to a glass. Finally, because the polymerization (at least to the same degree as in the liquid) is not retained in the gas phase, microwave and electron diffraction analyses are not applicable. Thus, this system illustrates nicely the type of structural problem best suited to NMR investigation.

Another class of octahedral structures whose stereochemistry was established by NMR is tungsten hexafluoride complexes with donor molecules, e.g., $WF_6{\cdot}(C_6H_5)_3P$ (*87a*). For these, the F^{19} spectra consist of a low-field doublet, a medium-field quintet and a high-field singlet of relative intensities 4:1:1. The doublet and quintet resonances establish the geometry

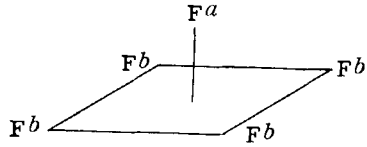

A heptacovalent structure cannot be devised to fit the NMR data because directed bonds from tungsten to both the donor ligand and the sixth fluorine

† Irrespective of end groups in a linear polymer.

atom would make the four fluorine atoms in the F^b set no longer equivalent. To preserve the required fourfold symmetry of the structure and also to account for the absence of FF coupling in the high-field singlet, an ionic octahedral model is proposed.

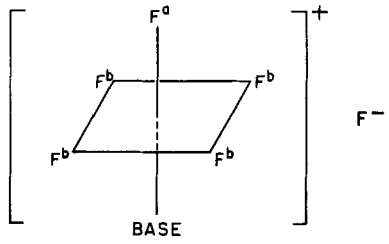

This model is consistent with the F^{19} spectrum and with the observation of electrolyte behavior for the complexes in a liquid sulfur dioxide medium.

C. Hydration Phenomena

A potentially very important application of NMR is the determination of solvation numbers for ions in solution. In aqueous systems there are, however, considerable difficulties in such applications. Proton resonances are unsuitable because of the extremely fast proton exchange between bound and unbound water. The O^{16} isotope does not possess a magnetic moment and, accordingly, cannot be observed in the NMR experiment. The O^{17} isotope does have a magnetic moment but is of very low natural abundance ($3.7 \times 10^{-2}\%$). Fortunately, O^{17} ($I = \frac{5}{2}$) also has a small nuclear quadrupole moment that is not large enough to broaden the nuclear resonances to the point that chemical shifts become nonobservable, but large enough to reduce T_1, the longitudinal relaxation time, and, permit use of large rf fields that would normally saturate spin levels of nuclei with $I = \frac{1}{2}$. Jackson *et al.* (*54*) have shown that separate O^{17} resonances are obtained in certain cases for bound and unbound water in electrolyte solutions. Integration, then, of the separate O^{17} resonances is an approach to direct determination of hydration numbers of ions. This application of NMR is limited by kinetic processes; the lifetime of water in the bound state must be greater than about 10^{-4} sec to prevent exchange broadening or coalescence of the individual resonances.

The O^{17} resonance of a saturated water solution of $[Co(NH_3)_5OH_2]Cl_3$* consists of two peaks; the O^{17} resonance of bound water is shifted to the high field side of solvent water. This shift unfortunately is of the same order

* The aquo cobalt salt was enriched in O^{17} by treatment with water containing 1.3% O^{17}; natural abundance of O^{17} is $3.7 \times 10^{-2}\%$.

of magnitude as the line widths and does not permit intensity determinations of very high accuracy. Jackson, Lemons, and Taube overcame this difficulty in elegant fashion by introducing a large paramagnetic solvent shift. This was achieved by adding a substantial concentration of the paramagnetic ion $Co(H_2O)_6^{++}$ which rapidly exchanges bound water with solvent water so that the observed O^{17} solvent shift is $\delta_{H_2O}[H_2O] + \delta_{Co(H_2O)_6^{++}}[Co(H_2O)_6^{++}]$. Because the rate of H_2O exchange between $Co(H_2O)_6^{++}$ and $[(NH_3)_5CoOH_2]^{3+}$ is "slow," there is no detectable shift in the O^{17} resonance of the bound water in the latter. This technique of inducing a large solvent shift is also of qualitative importance. For example, there is no detectable shift of O^{17} resonance between bound and unbound water in solutions containing Be^{++},Al^{3+}, and Bi^{3+} ions, but addition of paramagnetic ions such as Fe^{3+} and Co^{++} leads to solvent shifts of sufficient magnitude to permit resolution of separate resonances for solvent water and bound water.

The concentrations of O^{17} used in the work of Jackson, Lemons, and Taube proved too low for very accurate determination of hydration numbers. Water samples more highly enriched in O^{17} should provide the basis for important studies of solvation phenomena in solution.* This approach could be extended to other solvent systems such as liquid ammonia, amines, and acetonitrile (N^{14} or N^{15} resonances), ethers, sulfur dioxide, and dimethylsulfoxide (O^{17}), and BrF_3 (F^{19}).

D. Metal Hydrides

Abnormally large proton chemical shifts are encountered in transition metal hydrides, and these shifts have served as an excellent diagnostic test for the presence of metal-hydrogen bonds. Wilkinson and co-workers (*37, 38, 40, 70, 139*) have used the NMR approach to establish the existence of M—H bonds in a number of systems. Reduction of cyanorhodate(III) solutions was known to yield a unique anion, and this was presumed to be a cyanorhodate(I) species. However, Griffith and Wilkinson (*40*) found that the proton spectrum had a line shifted far to the high-field side of water. Since this high-field resonance is split into a doublet, its assignment to a hydrogen atom directly bound to rhodium is virtually unequivocal because Rh^{103} has a nuclear spin of $\frac{1}{2}$. Thus, the anion is an hydridorhodium(III) ion rather than a lower valent species. Similarly, reduction of cobalt(III) cyanides had been considered to yield cobalt(I) ions; the proton spectra of these and of aqueous cobalt(II) cyanide solutions show a high field resonance indicative of Co—H bonds (probably an $[HCo(CN)_5]^{3-}$

* Recently, Connick *et al.* (*16a, b*) have studied exchange reactions of water between the coordination sphere of transition metals and the solvent by O^{17} shifts.

anion). No fine structure due to $Co^{59} - H^1$ coupling is discernible, but this may reflect effects of Co^{59} relaxation through the interaction of the large Co^{59} quadrupole moment ($eQ = 0.5 \times 10^{-24}$) with the electric field gradient about cobalt.

The nature of the bonding of hydrogen in $(\pi\text{-}C_5H_5)_2ReH$ and $(\pi\text{-}C_5H_5)_2\text{-}ReH_2^+$ was elucidated by analysis of the proton spectra (*37*). Several models for the location of Re-H hydrogen atoms in these compounds had been proposed. For the neutral species, two possible structures are (I) and (II).

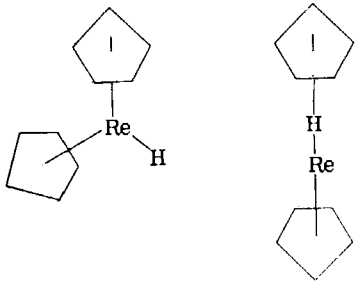

(I) (II)

The proton spectrum consists of a doublet C_5H_5 resonance and a high field Re-H peak. The doublet C_5H_5 resonances do not represent chemically-shifted resonances but $H_{C_5H_5}H_{Re}$ coupling, because in $(C_5H_5)_2ReD$ the C_5H_5 resonance is a singlet. The Re-H peak accordingly should be an eleven-line resonance but is, in fact, a broad structureless resonance. It is probable that the breadth of the proton resonance is attributable to the Re-H spin-spin interaction broadened by a short relaxation time of the rhenium nucleus ($I = 9/2$). These data are wholly consistent with Structure I.

In recent work, Wilkinson and co-workers have established from proton spectra that the M—H hydrogen atoms in $(\pi\text{-}C_5H_5)_2WH_3^+$ (*38*) and $(\pi\text{-}C_5H_5)_2TaH_3$ (*38*, *70*) are not equivalent. In the H^1 spectrum of $(\pi\text{-}C_5H_5)_2\text{-}TaH_3$ there is a low field singlet of intensity ten which was assigned to protons of the two C_5H_5 groups. There are also two high field resonances of relative intensities two and one which are respectively a doublet and a triplet* ($A_{HH} = 9.6$ cps) and these were assigned to TaH_2 and TaH groups. This somewhat surprising nonequivalence of MH hydrogen atoms in these

* There is some distortion of the triplet and doublet components. In this case $A_{H_2H_1}$ and $\nu_0\delta_{H_1H_2}$ are comparable, $A/\nu_0\delta = 1/8.2$, and perturbation of energy levels calculated from first order considerations is to be expected.

metal hydrides would have been rather difficult to establish by any other spectroscopic technique.

E. Organometallic Compounds

There are numerous cases of organometallic structure proof based on proton spectra. An interesting class within this group are the π-allyl metallics (*52, 57, 69, 128*). Allyl derivatives of transition metal carbonyls have been made, but these are for the most part rather unstable and readily lose carbon monoxide to form a new structure, e.g.,

$$\begin{aligned} NaMn(CO)_5 + C_3H_5Cl \rightarrow CH_2{=}CH{-}CH_2Mn(CO)_5 \\ \downarrow 50^\circ\ (-CO) \\ C_3H_5Mn(CO)_4 \end{aligned}$$

The proton spectrum of $CH_2{=}CHCH_2Mn(CO)_5$ is wholly consistent with a simple allylic structure (*69*) and will not be discussed here. In the case of $C_3H_5Mn(Co)_4$ the proton spectrum (*69*), shown in Fig. 6, requires a

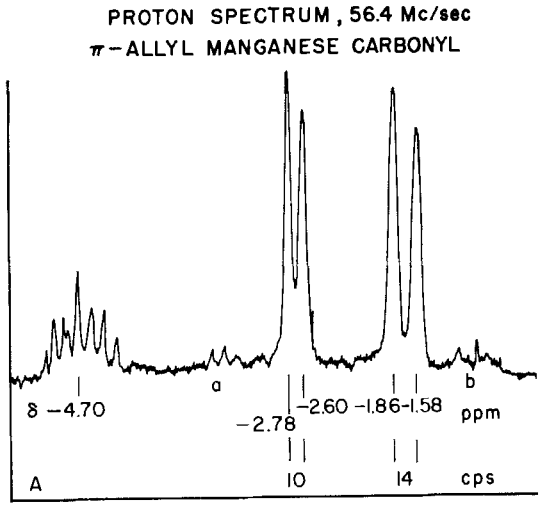

Fig. 6. Proton spectrum of π-$C_3H_5Mn(CO)_4$. Areas designated a and b are due to impurities. [McClellan *et al.* (*69*).]

structure with three distinct hydrogen-atom environments containing hydrogen atoms in the ratios 1:2:2; and this does not fit either an allyl or a vinyl structure for the ligand. Two possible structures that satisfy the inert gas consideration are

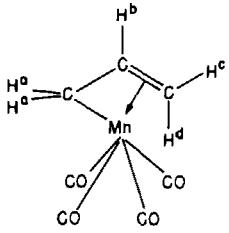

(I)

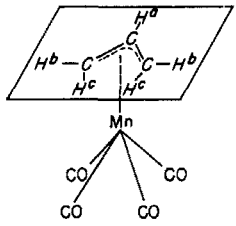

(II)

In (I) there are four hydrogen-atom environments, and this structure may be discarded. Structure (II), in which the allyl group is presumably planar, provides three environments for hydrogen atoms and is consistent with the proton spectrum. The two doublets represent the H^b and H^c hydrogen atoms. The seven-line multiplet represents the central hydrogen atom (this can be precisely reproduced by using the H^a—H^b and H^a—H^c coupling constants determined from the doublet separations). Spin coupling between H^b and H^c is vanishingly small and thus is consistent with the theoretical results of Karplus and co-workers (*45*) that suggest A_{HH} is very small where $\angle$HCH is near 120°. Further support of the π-allyl assignment is found in the H^1 spectra of allyl derivatives of cobalt (*69*), palladium (*23*, *69*, *128*) and nickel (*69*) which exhibit H^1 spectra qualitatively identical to that of the manganese compound. The H^1 spectra of substituted π-allyl derivatives (*58*, *69*) provide a final confirmation for a coplanar π-allyl ligand.

The proton spectrum of the allyl Grignard reagent consists of a quintet and a doublet of intensities one and four, respectively (*94*). Possible major Grignard species are:

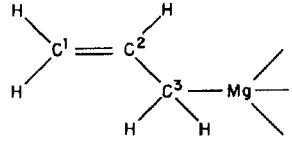

CLASSICAL MODEL

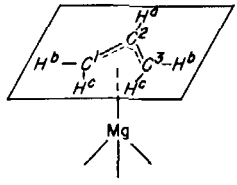

"SANDWICH" MODEL

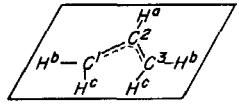

ION

None of these structures is consistent with the observed spectrum; some rapid dynamic process must exist which permits environmental exchange of the hydrogen atoms at C^1 and C^3. To attain equivalence, the "sandwich" model may be invoked as an exchange intermediate for the classical model if the latter is the major solution species, and vice versa. The NMR data do not, however, permit selection of any of these as the major solution species. The spectrum for a substituted allyl Grignard supports the classical formulation (*95*). This Grignard derived from either $CH_3CH{=}CHCH_2Br$ or $CH_3CHBrCH{=}CH_2$ exhibits a proton spectrum fully consistent with the butenyl structure

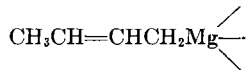

There is a CH_2 doublet in the region characteristic of aliphatic CH_2 resonances, a CH_3 doublet and two multiplets in the vinyl CH region. Since some rapid exchange process occurs in the allyl Grignard, it presumably also occurs here

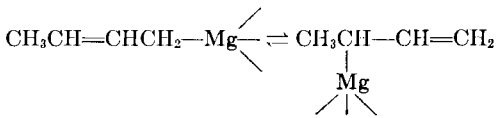

but the equilibrium must lie far to the left to account for the chemical shift data.

F. Boron Compounds

Boron compounds contain two isotopes B^{10} and B^{11} of natural abundances 19% and 81%, respectively. Although both these isotopes possess magnetic moments, the B^{11} nucleus is better suited to the high resolution experiment because of its (1) greater natural abundance, (2) smaller quadrupole moment, and (3) larger nuclear moment.* Because of the broad range of structures possible in boron compounds, particularly the hydrides, there has been considerable NMR work done in this field to confirm previously proposed structures and in a few cases to first establish geometry of a compound. The B^{11} spectra of tetraborane and a tetraborane derivative are considered below.

The structure of tetraborane had been established by X-ray analysis (*86*) (Fig. 7). Consistent with this structure the B^{11} spectrum (Fig. 8) comprises a low field triplet and a high field doublet of equal intensities (*117a, 138*). Splittings here reflect B^{11}—H^1 coupling since the H^1 spectrum

* With other things equal, the NMR signal-to-noise ratio increases with increasing nuclear moment.

consists of two overlapping quartets (for B^{11}, $I = 3/2$) of relative intensities one and two and a partially obscured bridge hydrogen resonance. Thus, the B^{11} triplet represents the B^aH_2 groups and the doublet, the B^bH groups.

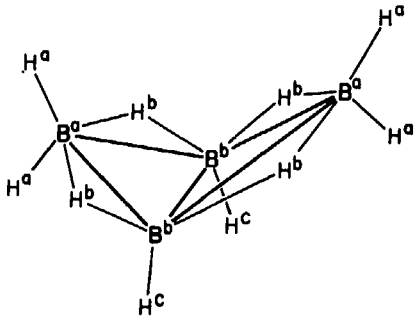

FIG. 7. Structure of tetraborane, B_4H_{10}. H^a and H^c represent the two types of terminal B-H hydrogen atoms and H^b the bridge B-H hydrogen atoms.

Tetraborane and ethylene react in a 1:1 ratio to form $B_4H_{12}C_2$ and hydrogen (*50*); the B^{11} and H^1 spectra permit a unique structural assignment to be made for the B_4 derivative (*124*). In the B^{11} spectrum, the low field triplet found in B_4H_{10} becomes a doublet and the high field doublet is unchanged. Thus, the B^a boron atoms now have only one terminal hydrogen

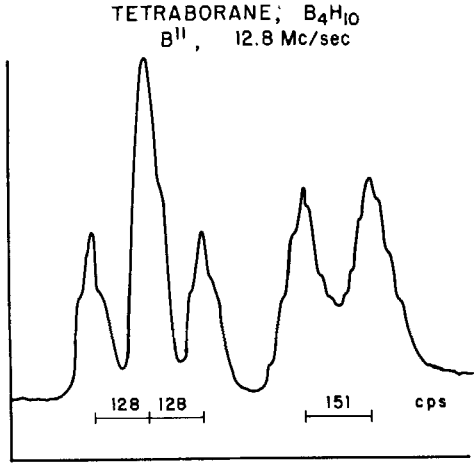

FIG. 8. B^{11} spectrum of tetraborane, B_4H_{10}. [Williams *et al.* (*138*).]

bond. The proton spectrum comprises a single sharp CH_2 resonance, a broad bridge hydrogen (H^b) resonance and two quartets for the terminal H^a and H^c hydrogen atoms. The only reasonable model consistent with these data is an ethylene bridged structure:

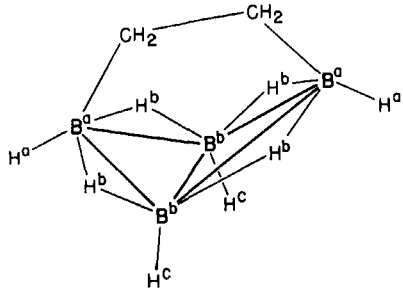

G. Other Nuclei

There have been many important studies based on resonances of nuclei other than those previously discussed; these include N^{14}, Na^{23}, P^{31}, Cl^{35}, Co^{59}, $Sn^{115, 117}$, and $Tl^{203, 205}$. Several of these studies are considered here because they illustrate two particular applications of NMR.

The Tl^{205} spectrum of Tl_2Cl_3 consists of two peaks of relative intensities one and three, and is consistent with the structure $(Tl^+)_3(TlCl_6^{3-})$ (*34*). The most interesting point here is that this spectrum is of Tl_2Cl_3 as a solid. Thus, chemically shifted nuclei can be detected in spectra of solids in apparent contradiction to the previously cited requirement that the compound be present in the gas, liquid, or solution state. In principle, chemical shifts can be resolved in spectra of solid compounds provided that the line widths, which are primarily governed by dipolar interactions in solids, are relatively small with respect to the separation between chemically shifted resonances. Recently, Andrew *et al.* (*3*) have described a sample spinning method for reducing resonance line widths in solids. They found that at a magnetic field of about 4740 gauss the P^{31} resonance of solid PCl_5 is broad and structureless. Broadening effects were reduced by an averaging of the dipole-dipole interactions through high speed rotation ($\geqq$800 rps) of the sample on an axis at an angle of 54°44′ to the direction of the magnetic field. Under these conditions, two equal intensity resonances were observed and this is the P^{31} spectrum expected for solid PCl_5 which is a tetragonal lattice composed of PCl_4^+ and PCl_6^- aggregates. This technique of high speed rotation of samples may greatly enlarge the scope of NMR stereochemical analysis by making some techniques of high resolution NMR applicable to solids.*

Attempts to isolate mixed halides of tin from mixtures of tin tetrahalides have been unsuccessful because of apparent rapid redistribution of halogen atoms. Existence of such mixed species has been suggested by extra lines ob-

* In a recent study (*26a*) Dreitlein and Kessemeier developed more completely the theory of NMR absorption by a mechanically rotating solid.

served in the Raman spectra of mixtures of $SnCl_4$ and $SnBr_4$ and of $SnCl_4$ and SnI_4. Burke and Lauterbur (*14*) have confirmed the existence of rapid equilibration among mixtures of $SnCl_4$, $SnBr_4$, and SnI_4 and quantitatively described these systems from a study of the Sn^{119} spectra of such mixtures; e.g., the Sn^{119} spectrum of a $SnCl_4$:$SnBr_4$ mixture consists of five resonances—two are attributable to $SnCl_4$ and $SnBr_4$ and the remaining three, nearly equally spaced between the outer two lines, arise from $SnCl_3Br$, $SnCl_2Br_2$, and $SnClBr_3$. The intensities of the five lines are those expected for a redistribution reaction in which all five species have equal thermodynamic

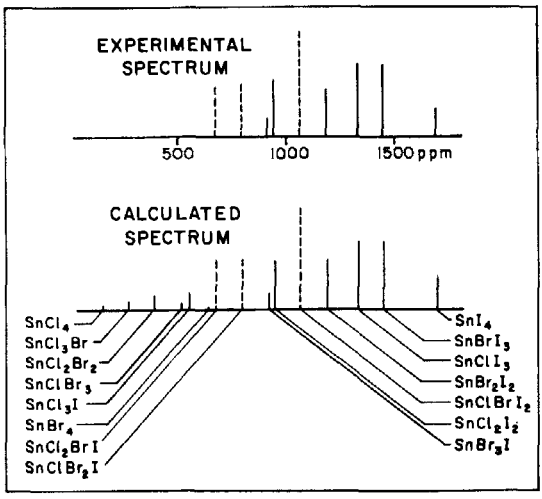

FIG. 9. Experimental and theoretical spectra for a 2:1:1 molar mixture of SnI_4, $SnBr_4$, and $SnCl_4$. Dotted lines represent the three new peaks for the new species $SnCl_2BrI$, $SnClBr_2I$, and $SnClBrI_2$. [Burke and Lauterbur (*14*).]

stability. This random distribution was further substantiated by varying the proportions of the pure halides and following intensity changes of Sn resonances for the various species. Similar behavior was found for the $SnCl_4$-SnI_4 and $SnBr_4$-SnI_4 systems. Finally the ternary system $SnCl_4$, $SnBr_4$, and SnI_4 was examined. The observed spectrum for a 2:1:1 molar mixture of SnI_4:$SnBr_4$:$SnCl_4$ agreed fairly well with the calculated spectrum, assuming random distribution of halogen atom among all possible species (Fig. 9).

A similar analysis of mixed boron halides from F^{19} spectra of the BF_3—BCl_3—BBr_3 system has been made by Coyle and Stone (*20*), and the existence of all possible mixed species was established.

H. Some Sources of Interpretational Error

Interpretation of NMR spectra is subject to the same types of errors encountered in other spectroscopic analyses. There are, however, several pitfalls unique to NMR that may not be avoided if all the factors that can affect resonance-line shape are not clearly understood. These factors are considered here to emphasize the need for care in interpretation.

The most serious and probably most common error is encountered in conclusions based *solely* on the observation of a single-line resonance. In itself, such an observation permits only one conclusion: there are magnetic nuclei present in the sample. This may seem an exceedingly cautious position; however, there are several distinct processes through which environmentally nonequivalent nuclei can be rendered spectroscopically equivalent. Furthermore, processes characterized by rather low rates (10^1 to 10^3 sec^{-1}) often can be responsible for effective averaging in the NMR experiment. Unless the absence of such processes can be established directly or indirectly, the single-line resonance is stereochemically meaningless. Factors which can affect line shape are considered separately in the following sections.

I. Intermolecular Exchange

The F^{19} spectrum of $TiF_4 \cdot 2C_2H_5OH$ is a single-line resonance at room temperature. This observation would suggest the structure is *trans* octahedral as would be expected from purely electrostatic or steric considerations. In fact, however, the geometry is *cis* and the expected pair of triplets arising from this structure is not observed unless the sample is cooled to 0° or below (*87*). Spectroscopic equivalence of fluorine atoms in this compound results from a chemical exchange process involving alcohol molecules that results in environmental exchange of fluorine atoms between the two nonequivalent sites.

$$TiF_4 \cdot 2C_2H_5OH \rightleftharpoons C_2H_5OH + TiF_4 \cdot C_2H_5OH$$

Only when the rate of alcohol exchange is lowered by cooling is the nonequivalence of fluorine atoms evident in the NMR spectrum. These exchange effects are observed because at room temperature the chemical shift* between fluorine atoms in the two environments is comparable to the exchange rate. Chemical shifts† and coupling constants of nuclei in molecules are comparable to the rates of many chemical processes. Consequently this possible "complication" must always be kept in mind. Exchange phe-

* At 40 Mc/sec.

† Expressed in frequency units.

nomena themselves are an important area of NMR investigation and are treated in the following section of this chapter.

Exchange collapse of multiline spectra has been observed in a large number of inorganic compounds, e.g., SF_4 (*18, 89*), SbF_5 (*53*), ClF_3 (*49, 88a*), $BF_3 \cdot 2C_2H_5OH$ (*25*), and $B_2H_5N(CH_3)_2$ (*104*). Such effects are to be especially anticipated in unstable or highly reactive compounds. In these cases the spectra must be examined as a function of temperature. It may not always be possible to lower exchange rates sufficiently by cooling because of experimental complications. Alternatives are (1) to employ for resonance the maximum possible rf frequency (or magnetic field) to increase the chemical shift, and (2) dilution with inert solvents to reduce intermolecular exchange rates. Purity is also a consideration in that trace impurities may catalyze the exchange process. For example, the expected triplet (N^{14}—H coupling) proton spectrum for ammonia is observed only if the last traces of water are removed with sodium metal (*96*). This purity consideration is especially relevant for inorganic fluorides in that traces of F^- or HF can often catalyze fluorine exchange.

Line shape changes due to intermolecular exchange processes can also be minimized or even eliminated by reducing the concentration of the exchange intermediate by chemical complexing. For example, the triplet proton spectrum expected for NH_4^+ is observed only at low pH where ammonia, the principal intermediate in proton exchange between NH_4^+ and H_2O, is at very low concentration (*97*). Recently, a striking application of this type was reported by MacLean and Mackor (*80*). They observed the proton singlet for H_3O^+ and the triplet for the H_2O^+ group in $^+H_2OCH_2CH_3$ in acidified ethanol. Here, concentrations of the principal proton exchange intermediates, water and ethanol, were reduced by addition of excess strong acid, HBF_4.

In some instances, structural conclusions based on single-line resonances may be justified if there are supporting data. A case in point is that of the sulfur(VI)fluorides (*89a*). In the monomeric compound

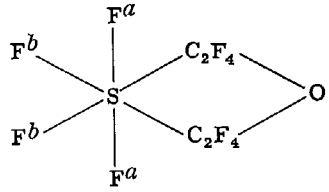

the CF_2 groups are obviously *cis* and the S—F resonances do consist of the expected pair of triplets; the F^a—F^b chemical shift is large, 28.2 ppm. The closely-related compounds, $(C_2F_5)_2SF_4$ and $(C_3F_7)_2SF_4$, have single S—F resonances. In these cases, a *trans* structure is strongly indicated

since the established *cis* structure has a very large F^a—F^b shift and since fast exchange processes in these nonreactive molecules are very unlikely. Other evidence for large F^a—F^b shifts in *cis* octahedral SF_4A_2 structures comes from the spectrum of $SF_4(SO_3F)_2$ (*15*). The part of the spectrum

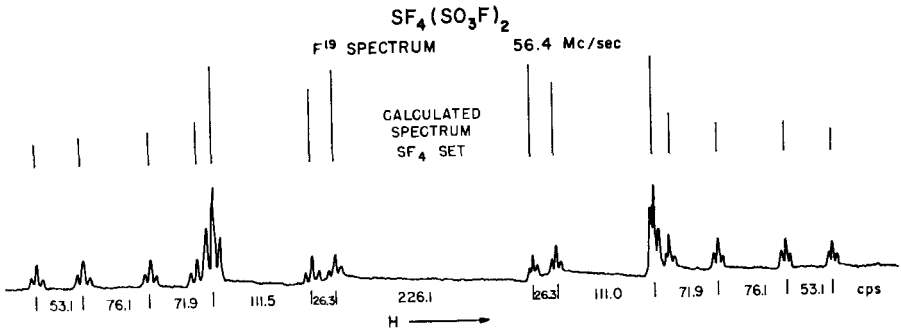

FIG. 10. Experimental and calculated F^{19} spectra of $SF_4(SO_3F)_2$. Only that part of the spectrum arising from the SF_4 fluorine atoms is reproduced. The recurring triplet fine structure is due to F-F coupling between SF_4 fluorine atoms and SO_3F fluorine atoms. [Cady and Shreeve (*15*).]

arising from the SF_4 set (Fig. 10) is complex, indicating that higher order effects must be taken into consideration. This A_2B_2* situation for the *cis* configuration has been solved and analysis yields values of 9.1 ppm for $\delta_{F^a-F^b}$ and 156 cps for $A_{F^a-F^b}$.

J. Intramolecular Exchange via Classical Processes

Intramolecular exchange based on rotational or vibrational processes can in principle also lead to effectively averaged environments in the NMR experiment. Rotational exchange is often encountered in organic compounds; in particular, striking examples are found in spectra of substituted ethanes, amides, and nitrites, and these have been treated in detail in the original literature (*105*) and in reviews (*102, 110, 120*). No examples of this type of exchange in inorganic compounds have as yet been established; however, this may be the explanation for an anomaly found in the F^{19} spectra of phosphorus(V) fluorides. Phosphorus pentafluoride has trigonal bipyramid symmetry (*12, 13*), but the F^{19} spectrum is a single, sharp resonance (*47*). A similar situation obtains in a large number of monosubstituted derivatives which include CH_3PF_4, i-$C_8H_{15}PF_4$, $C_6H_5PF_4$, and $CH_3C_6H_4PF_4$ (*123*). Apparent environmental equivalence cannot in these cases be the result of intermolecular fluorine exchange because P^{31}—F^{19} coupling is preserved, and all these spectra are invariant over fairly broad

* See reference *109* for terminology used in classification of NMR spectra.

temperature ranges, $\sim -100°$ to $+150°$. Intramolecular exchange based on a vibrational process would not involve P—F bond breaking and could account for the spectroscopic equivalence of fluorine atoms. Berry (*6*) has considered this possibility in some detail and suggested a specific mechanism for PF_5. Interestingly, several other compounds that have trigonal bipyramid geometry show spectroscopic equivalence of ligand atoms or groups. These are $Fe(CO)_5$[C^{13} NMR] (*11a*, *17b*), VF_5 (*15a*) and AsF_5 (*88*, *89*) [F^{19} NMR].

K. Quadrupole Interaction

Other effects frequently encountered in inorganic systems that can severely affect line shape involve relaxation processes arising from interactions of nuclear quadrupole moments with electric field gradients. For quadrupolar nuclei ($I \geqslant 1$), the quadrupolar contribution to the spin-lattice relaxation time T_1 is given approximately by

$$1/T_1 = (3/8)\hbar^2\tau_c(eq)^2(eQ)^2 \tag{26}$$

where eq is the field gradient, eQ the nuclear quadrupole moment and τ_c the correlation time for rotational motion of the molecule in the liquid. The correlation time may be approximated from the expression for an idealized spherical model

$$\tau_c = \frac{4\pi\eta a^3}{3RT} \tag{27}$$

where η is the macroscopic viscosity and a is the radius of the sphere. From Eq. (26), it can be seen that if the quadrupole coupling constant is large, T_1 is small. The NMR line width, to which T_1 contributes, will therefore be large. In a symmetrical environment where the field gradient is zero or very small, there should be no significant line broadening from quadrupolar effects.

In NMR investigations of nuclei that possess quadrupole moments, the possible consequences of quadrupole interaction must always be considered. Apparent spectroscopic equivalence of environmentally nonequivalent nuclei may arise in special instances. For example, in a molecule for which a given nucleus of spin $\geqslant 1$ may reside in two nonequivalent environments, the quadrupole coupling constant in one environment may be small and in the other very large. For the latter environment, the line broadening due to quadrupole relaxation may be so great as to make the resonance indistinguishable from the background.

A possible example of this behavior is encountered in the N^{14} resonance spectrum of azoxybenzene. Since two N^{14} resonances are observed for N,N-dimethylnitrosamine (*101*) and three N^{14} resonances are observed for

benzylazide (*101*), it was to be expected then that the two structurally nonequivalent nitrogen atoms of azoxybenzene would exhibit two well separated resonances. However, only one N^{14} resonance is observed (*101*). As was first suggested by Orgel (*99*), it is possible that the electric field gradient experienced by N^a may be so large as to make its

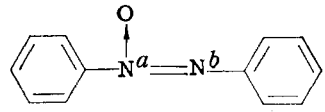

resonance practically nonobservable. In a possibly related example, one isomer of N_2F_2 is thought to have one of two structures (*28*):

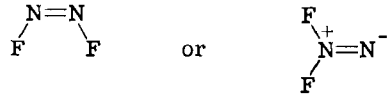

(I) (II)

It is generally agreed that the second isomer has the *trans* structure (III) (*28*):

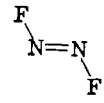

(III)

Single N^{14} resonances are observed for both isomers (*16*). This suggests that (I) is the correct structure of the isomer of disputed structure. While this may be so, the azoxybenzene example cautions restraint in basing proof of structure on this evidence alone.

All nuclear multiplet structures due to coupling of nonequivalent nuclei are, as noted earlier, subject to effects on line shapes by chemical or positional exchange. For those multiplet structures arising from coupling of nuclei, one of which has a nonzero nuclear quadrupole moment, effects of quadrupole relaxation must be considered. For example, if a proton or fluorine atom is bonded to a nitrogen nucleus ($I = 1$), a triplet resonance will be expected in the proton or fluorine spectrum. For observation of this fine structure it is necessary that the lifetimes of the nuclear spin states of nitrogen ($m = 1, 0, -1$) be greater than the inverse frequency separation between multiplet components, i.e., $\tau > 1/A_{NX}$ (*106*). The lifetimes of N^{14} spin states can become comparable to or less than $1/A$ as a result of quadrupole relaxation. When the N^{14} spin-state lifetimes are comparable

to or less than $1/A$, the F^{19} or H^1 multiplet structure disappears and a single resonance appears. Here, transitions between N^{14} spin states have become so rapid that the multiplet structure on F^{19} or H^1 no longer is observable. Molecular correlation time increases with temperature decrease [Eq. (27)] and an increase in correlation time decreases the effectiveness of the relaxation process. Thus, transitions from singlet to multiplet spectra will follow temperature increase rather than the inverse sequence found in processes reflecting chemical or positional exchange. In Fig. 11, the tem-

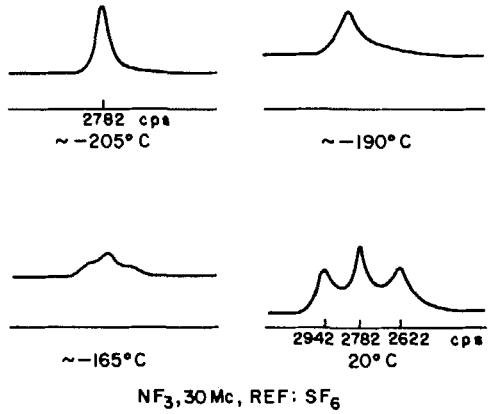

FIG. 11. Temperature dependence of the F^{19} spectrum of NF_3 [Muetterties and Phillips (*89*).]

perature dependence of the F^{19} spectrum of NF_3 is reproduced. For this particular case, at the temperature of $\sim -180°$ where the triplet structure disappears, the lifetime of a given N^{14} spin-state approximates $(\frac{5}{2}\pi A_{NF})$ or 10^{-3} sec (*89*). This phenomenon connected with quadrupolar nuclei again demonstrates the importance of examining spectra as a function of temperature.

L. Nonclassical Exchange Processes

Apparent NMR equivalence of nuclei can also arise by a quantum mechanical intramolecular tunneling process. In principle, this process may be differentiated from intermolecular exchange processes because although the exchanging nuclei are rendered equivalent insofar as the NMR experiment is concerned, spin-spin splitting by other magnetic nuclei is not washed out. This type of intramolecular exchange is manifested in several boron hydride derivatives. It was first proposed by Ogg and Ray (*98*) to explain the NMR spectra of aluminum borohydride, whose structure is

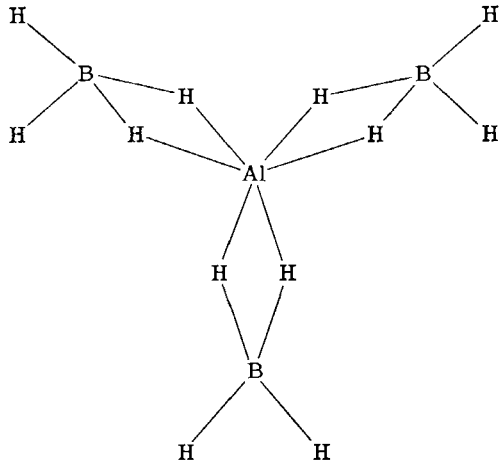

The proton spectrum consists of a single broad line, presumably due to broadening effects arising from the quadrupolar Al^{27} nucleus. Spin coupling of H^1-Al^{27} can be eliminated by a saturating field at the Al^{27} resonance frequency and the resulting H^1 spectrum is a quartet suggesting that all protons are environmentally equivalent and equally coupled with the boron nucleus (B^{11}, $I = 3/2$). Consistent with this picture, the B^{11} spectrum comprises the quintet expected for equal coupling with the four protons. There is no intermolecular process that will produce equivalence of hydrogen atoms and yet retain H^1—Al^{27} and H^1—B^{11} coupling. The only process consistent with the data is an intramolecular quantum mechanical tunneling through the potential barriers to BH_4 rotation. This mechanism would not break the H^1—Al^{27} coupling and would only demand a frequency of tunneling greater than the NMR frequency separation of the bridge and terminal hydrogen atom positions. In diborane, the bridge-terminal shift is 4.3 ppm. Accordingly, the frequency of tunneling must be greater than about 10^3 cps (at 30 Mc/sec).

A similar situation is found in the H^1 and B^{11} spectra of $B_3H_8^-$. X-ray studies show this anion to have the boron atoms at the corners of an isosceles triangle.

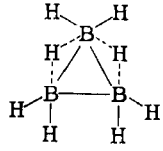

The B^{11} spectrum is a symmetrical nine-line pattern with intensity ratios in close agreement with that expected for eight hydrogen atoms equally

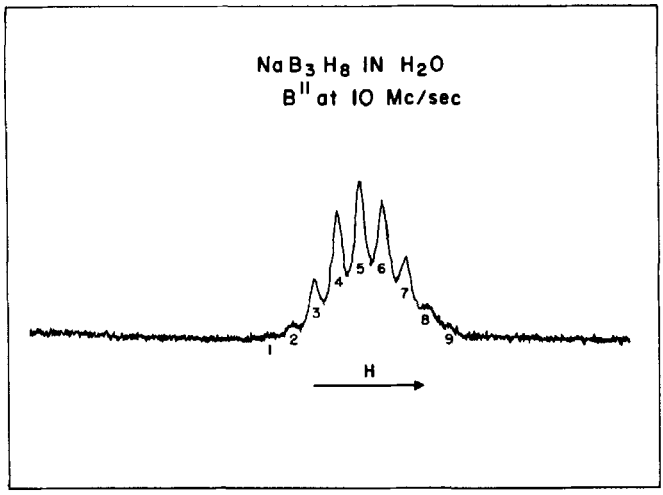

FIG. 12. B^{11} spectrum of an aqueous solution of NaB_3H_8. A_{BH} is 32 cps. [Miller (*85*).]

coupled to each of the three boron atoms (Fig. 12). In agreement with this picture, the proton spectrum is a decet with proper intensity ratios for three B^{11} atoms equally coupled to each hydrogen atom (Fig. 13). The original work (*104*) reported a septet B^{11} spectrum and a diffuse H^1 spectrum. With

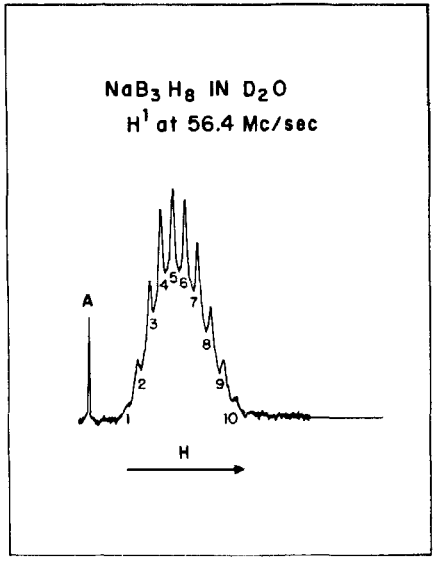

FIG. 13. Proton spectrum of $Na_3B_3H_8$ in D_2O. Area A is a water resonance due to trace amounts of water in the sodium salt. [Miller (*85*).]

sample purification, the spectra reproduced in Figs. 12 and 13 were obtained (*85*). The most likely explanation of the H^1 and B^{11} spectra of $B_3H_8^-$, first proposed by Lipscomb (*67*), again appears to be a tunneling process.

IV. Exchange Phenomena

A. Introduction

In NMR, the resonance frequency separations between nuclei in nonequivalent environments and between nuclear spin hyperfine components are comparable to the rates of many chemical processes. Thus, resonance characteristics can be profoundly affected by a variety of inter- and intramolecular rate processes. This area of application of NMR is exceedingly important for it provides a straightforward approach to studies of many exchange reactions. In the NMR measurement, there is no perturbation or consumption of sample. Temperature control and line-width or line separation measurements are the limiting factors in the precision. Most importantly, this approach can be applied to fast chemical or exchange reactions that in many cases could not be analyzed or could be analyzed only with extreme difficulty by other existing techniques. These are exemplified by the exchange processes, first detected and studied by NMR analyses, in such systems as $(SbF_5)_x$[53], allyl Grignard reagent[94], thallium alkyls[81] and SF_4[18].

Changes in nuclear resonance characteristics due to exchange processes may be described fairly accurately. Consider a hypothetical molecule in which there are two proton environments, each containing equal numbers of hydrogen atoms. The H^1 resonance spectrum (assume $A_{H_AH_B} \rightarrow 0$) will then consist of two peaks of equal intensity separated by some chemical shift $\nu_A^\circ - \nu_B^\circ$

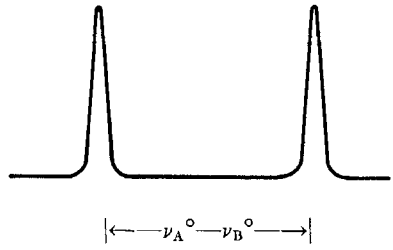

If, by heating or catalysis, exchange of hydrogen atoms between environments A and B occurs, and if the exchange rate τ^{-1} (where τ is an average time between exchanges) is large with respect to $\nu_A^\circ - \nu_B^\circ$ [$\tau^{-1} > 10(\nu_A^\circ - \nu_B^\circ)$], the spectrum will consist of a single peak centered at a position midway between ν_A° and ν_B°.

The transition region between "slow" and "fast" exchange has been

described by Gutowsky *et al.* (*47*), Gutowsky and Holm (*44*), and McConnell (*73*) for the above case by solution of modified Bloch equations that take into account the possibility of exchange between environments A and B. With the simplifying assumptions of equal numbers and lifetimes of hydrogen atoms in environments A and B, and large transverse relaxation times ($1/T_{2A} = 1/T_{2B} = 0$), a line shape function $g(\nu)$ may be derived.

$$g(\nu) = K \frac{\tau(\nu_A^\circ - \nu_B^\circ)^2}{[\frac{1}{2}(\nu_A^\circ + \nu_B^\circ) - \nu]^2 + 4\pi^2\tau^2(\nu_A^\circ - \nu)^2(\nu_B^\circ - \nu)^2} \tag{28}$$

where K is a normalizing constant and τ is the lifetime of a hydrogen atom in environment A or B. The plots of the function in the transition region

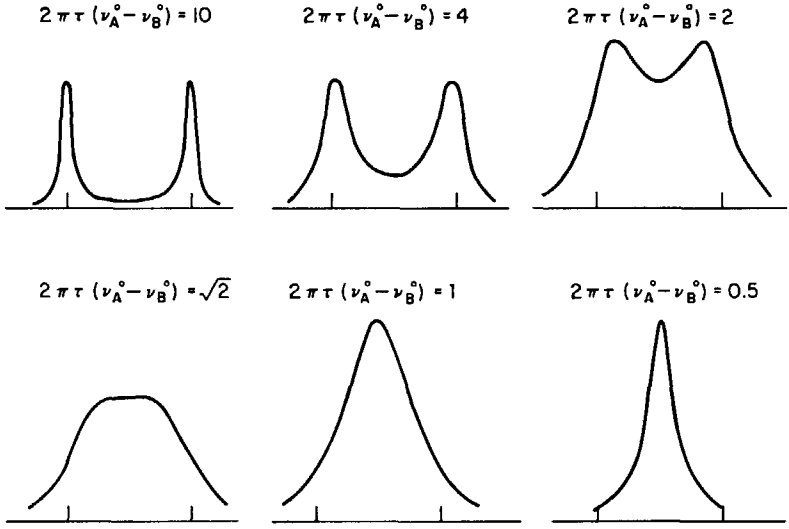

FIG. 14. Plot of line shape change versus rate of exchange of protons between environments A and B. The intensities of the various line functions are not comparable. Reproduced by permission from "High-Resolution Nuclear Magnetic Resonance," by Pople, Schneider, and Bernstein. McGraw-Hill, New York, 1959.

are shown approximately in Fig. 14. Thus it can be seen that as $\tau \rightarrow 1/(\nu_A^\circ - \nu_B^\circ)$, the individual peaks broaden and begin to merge. At

$$\tau = \frac{1}{\sqrt{2}\pi(\nu_A^\circ - \nu_B^\circ)} \tag{29}$$

the peaks merge into a single broad resonance, and then progressively sharpen with further decrease in the lifetimes. Analysis by line shape function is applicable to any part of the exchange region; however, line-shape analysis is a tedious process. If certain conditions are met, the

exchange analysis may be greatly facilitated. These special cases are considered in the following paragraphs.

From Eq. (28), a relation between the chemical shifts and the lifetimes may be derived:

$$\frac{\nu_A - \nu_B}{\nu_A^\circ - \nu_B^\circ} = \left[1 - \frac{1}{2\pi^2\tau^2(\nu_A^\circ - \nu_B^\circ)^2}\right]^{1/2} \tag{30}$$

or

$$\tau = \frac{1}{\sqrt{2}\pi}[(\nu_A^\circ - \nu_B^\circ)^2 - (\nu_A - \nu_B)^2]^{-1/2} \tag{31}$$

where $\nu_A - \nu_B$ represents the resonance separations under conditions of exchange. These equations are suitable only for analysis of that part of the transition region in which separate resonances for H_A and H_B are observed, and only if the separations are large with respect to the line widths. In some cases, this transition region may not be accessible either because (1) the rate is too low for complete coalescence of the components within the experimentally limited temperature range or (2) the rate is too high for separation into individual components by cooling. If the "fast" or "slow" areas of the transition region can be approached experimentally, these may be analyzed by line-width measurements. In the case of slow exchange, the broadening of components is related to lifetimes.

$$1/T'_{2A} = 1/T_{2A} + 1/\tau_A \tag{32}$$

$$1/T'_{2B} = 1/T_{2B} + 1/\tau_B \tag{33}$$

These equations are identical if the lifetimes in environments A and B are equal. T_2 and T'_2 are the transverse relaxation times in the absence of exchange and the presence of exchange, respectively, and are inversely related to the line widths.

As noted before, very rapid exchange leads to complete collapse to a single resonance which is located between ν_A° and ν_B°. The position of the resonance is at $p_A\nu_A^\circ + p_B\nu_B^\circ$ where p represents the fraction of resonating nuclei in a given environment. If the exchange is not sufficiently fast to give complete collapse, the line width will be given by Eq. (34) in which the lifetimes τ_A and τ_B are related to line broadening.

$$1/T'_2 = \frac{p_A}{T_A} + \frac{p_B}{T_B} + 4\pi^2 p_A^2 p_B^2(\nu_A^\circ - \nu_B^\circ)^2(\tau_A + \tau_B) \tag{34}$$

Use of Eqs. (32), (33), or (34) for determination of τ requires an independent determination of T_2's, the transverse relaxation times in the absence of exchange.

The above equations are limited to treatment of exchange between two environments; the general analysis for n environments has been described in detail by Anderson (*2*), Kubo (*64*), and Sack (*121*).

B. Proton Exchange

The H^1 spectra of compounds in which hydrogen atoms are directly bonded to a nitrogen atom consist of a triplet in the absence of fast exchange. Any exchange process that involves fast N—H bond breaking will then destroy this coupling. Experimentally, this effect has been observed for proton exchange between NH_4^+ and H_2O. The triplet proton spectrum of, for example, an aqueous NH_4Cl solution broadens with increase in pH and ultimately collapses to a single peak. Meiboom *et al.* (*84*) have studied this system by analysis of component broadening in the "slow" exchange region Eq. (32)]. This "slow" region comprises a relatively broad range of exchange rates because A_{N-H} is $\sim$1 cps. In this kinetic analysis, four contributing mechanisms to proton exchange were considered:

(a) $$NH_4^+ + H_2O \xrightarrow{k_a} NH_3 + H_3O^+$$

(b) $$NH_4^+ + OH^- \xrightarrow{k_b} NH_3 + H_2O$$

(c) $$NH_4^+ + NH_3 \xrightarrow{k_c} NH_3 + NH_4^+$$

(d) $$NH_4^+ + \overset{H}{\underset{|}{O}}\text{—}H + NH_3 \xrightarrow{k_d} NH_3 + H\text{—}\overset{H}{\underset{|}{O}} + NH_4^+$$

The contribution of reaction (a) to the H^1 line width may be estimated from the line width at very low pH where $[OH^-]$ and $[NH_3]$ are very small and accordingly k_b, k_c, and k_d are relatively unimportant. This sets an upper limit to k_a of $<0.6 \times 10^{-2}$ sec^{-1} M^{-1} at 21°. Since the analysis of exchange was studied in the pH range 1.5–2.5, reaction (b) is relatively unimportant because $[OH^-]$ is very small and the upper limit for k_b was estimated to be 10^{-12} sec^{-1} M^{-1}. Thus, under these experimental conditions, only k_c and k_d contribute significantly to the overall exchange broadening, and these are related to τ, the proton lifetime in a given NH_4^+ ion by Eq. (35).

$$\frac{4}{\tau_N} = \frac{2}{3} k_c + k_d^* \tag{35}$$

Separate values for k_c and k_d may be obtained by analysis of the broadening of the water proton resonance; since only reaction (d) contributes to this process, Eq. (36) holds.

* Proton exchange between nitrogen atoms in the same spin state does not affect line shape and since there are three spin states for nitrogen, only 2/3 of the proton transfers in reaction (c) contribute to line broadening.

$$k_d = \frac{2[H_2O]}{[NH_4Cl]} \frac{1}{\tau_W} \tag{36}$$

Evaluation of τ_W and τ_N yield

$$k_c = 10.6 \pm 1.0 \times 10^8 \text{ sec}^{-1} M^{-1} \text{ at } 21°$$

$$k_d = 0.9 \pm 1.0 \times 10^8 \text{ sec}^{-1} M^{-1} \text{ at } 21°$$

A more detailed treatment of proton exchange in NH_4^+ has been described in two recent articles (*17*, *27*). Similar analyses of proton exchange for R_3NH^+, $R_2NH_2^+$, and RNH_3^+ have been made by Grunwald *et al.* (*41–43*), and Lowenstein and Meiboom (*68*).

C. Exchange of Alkyl Groups in Organometallic Compounds

Rapid exchange of alkyl groups occurs in thallium(III) alkyls as demonstrated by the proton NMR study of Maher and Evans (*81*). At low temperatures ($\sim -85°$) the multiplet structure expected for proton-thallium coupling is superimposed on the proton spectra of thallium alkyls. On warming, the multiplets collapse. Analysis of this collapse region [Eq. (29)] yielded a value of 6 ± 1 kcal mole^{-1} for the exchange-activation energy

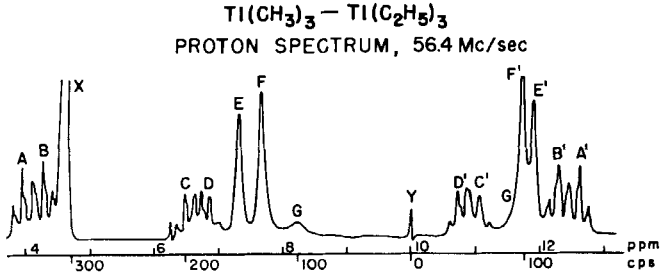

FIG. 15. Proton spectrum of a dichloromethane solution of $Tl(CH_3)_3$ and $Tl(C_2H_5)_3$ at $-85°$. Assignments were made to individual groups by following intensity changes with variation of the $Tl(CH_3)_3/Tl(C_2H_5)_3$ ratios. Thallium-203 and -205 isotopes have spin of 1/2 so each alkyl proton resonance is widely split into a doublet. Assignments are $Tl(CH_3)_2C_2H_5$: A,A′, CH_3 of C_2H_5 group; C,C′, CH_2, and FF′, CH_3 groups; $Tl(CH_3)(C_2H_5)_2$: B,B′, CH_3 of C_2H_5 group; D,D′, CH_2, and G,G′, CH_3 groups; $Tl(CH_3)_3$, E,E′. The resonances at X and Y are for dichloromethane and tetramethylsilane, respectively. [Maher and Evans (*81*).]

in $Tl(CH_3)_3$ in dichloromethane. It was further shown that in a mixture of $Tl(CH_3)_3$ and $Tl(C_2H_5)_3$ there is rapid exchange of alkyl groups, and resonances for $Tl(CH_3)_2C_2H_5$ and $TlCH_3(C_2H_5)_2$ as well as those for $Tl(CH_3)_3$ and $Tl(C_2H_5)_3$ were observed at $\sim -85°$ (Fig. 15). In similar fashion, Muller and Pritchard (*91*) have shown that fast exchange of methyl groups occurs in the trimethylaluminum dimer. Here the exchange

activation energy is 6–12 kcal mole^{-1}, significantly less than the heat of dissociation of the dimer, 20 kcal mole^{-1}. Thus, Muller and Pritchard concluded that the exchange mechanism is not dimer dissociation but some type of intramolecular process.

D. Fluorine Exchange

Examples of kinetic analysis of NMR spectra in the transition between "slow" and "fast" exchange (on the NMR time scale) are somewhat limited. Treatment of fluorine exchange in sulfur tetrafluoride is selected here because this exchange process exemplifies the type of kinetic process ideally suited to NMR study. The fluorine atoms of the two nonequivalent environments in this molecule of C_{2v} symmetry give rise to two triplets under conditions of very slow exchange at temperatures below $-85°$ (at 40 Mc/sec).

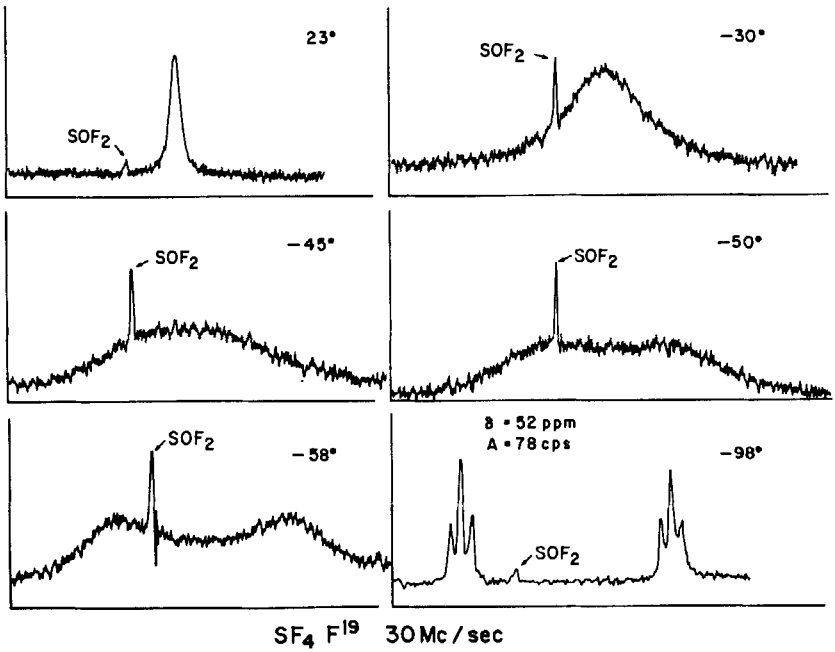

Fig. 16. Temperature dependence of the F^{19} spectrum of SF_4. [Muetterties and Phillips (*89*).]

As the temperature of the system approaches $-85°$, the triplet fine structure broadens and finally merges. Then these two peaks broaden with further temperature increase and finally merge at about $-45°$; this single broad peak then progessively sharpens with further temperature increase. The F^{19} spectra of SF_4 in the temperature range -98 to $23°$ are pre-

sented in Fig. 16. Cotton *et al.* (*18*) determined an average activation energy of 4 ± 1 kcal mole^{-1} for this exchange process by calculation of the fluorine atom lifetimes at the temperatures of triplet collapse and coalescence of chemical shifts [Eq. (29)]. In another analysis of the exchange in SF_4 (*89*), the separations between the chemically shifted peaks in the transitional region were substituted into Eq. (30). Results of this analysis are presented graphically in Fig. 17, and the activation energy derived from this plot is 4.5 ± 0.8 kcal mole^{-1}, which is in good agreement with the determination of Cotton, George, and Waugh.

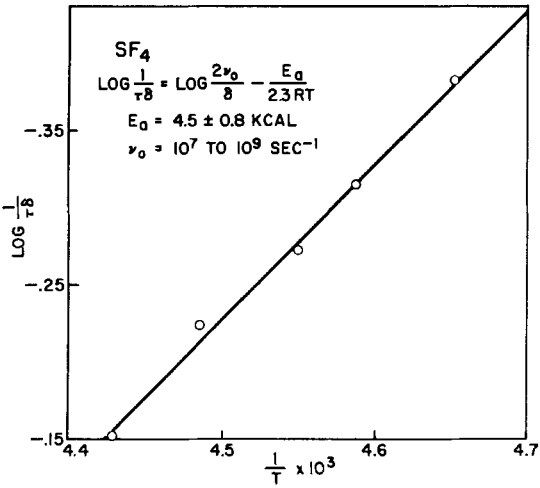

FIG. 17. Determination of E_a and ν_0 for fluorine exchange in SF_4 where ν_0 here is the frequency factor and δ is the chemical shift in cps. [Muetterties and Phillips (*89*).]

Possible reaction mechanisms may be eliminated in some cases by NMR studies. This has been done in the case of fluorine exchange in SF_4 (*89*) and it is perhaps worthwhile to consider the simplicity of such determinations. First, a wall reaction was ruled out by adding finely divided glass fragments to the sample; this increase in wall area by at least a factor of 10^2 did not detectably affect the exchange rate. Differentiation between an inter- and intramolecular process was made by examining the exchange rate as a function of SF_4 concentration in inert solvents; here the rate was markedly lowered on dilution, clearly indicating an intermolecular exchange. Of the three possible intermolecular processes, ionization, association, and dissociation(radical), the last was readily eliminated. In such a radical scheme, F· is produced and this radical is so reactive that if organic molecules are present an irreversible fluorination must take place; fluorination was not observed when SF_4 was in contact with a variety of organic compounds.

Final choice between an ionization and association mechanism was not reached in this case.

In principle, NMR could provide information about an actual exchange intermediate. For this, the intermediate must, in order to be detected, have a substantial lifetime and be present in rather appreciable concentration. An example that perhaps comes close to this situation is to be found in the F^{19} spectrum of antimony pentafluoride. As noted in the Stereochemistry section (p. 248) this fluoride is polymeric at low temperatures. This association is achieved through *cis* fluorine bridges. The three chemically shifted components of the F^{19} spectrum of $(SbF_5)_x$ observed below 15° undergo exchange collapse near room temperature (*53*). Here exchange may be adequately described as a dissociation based on the breaking and reforming of bridge bonds.

E. Kinetics of Triiodide Formation

The I^{127} NMR absorption line of covalently bound iodine is so broad that it has not yet been observed. This breadth is due to the short relaxation time of the I^{127} nucleus which possesses a large nuclear quadrupole moment ($eQ = 0.59 \times 10^{-24}$ cm^2). If, however, the field gradient seen by the I^{127} nucleus is vanishingly small as in the case of the spherically symmetrical iodide anion, the broadening effect is correspondingly small or zero because line width is proportional to the product of the squares of the field gradient and the quadrupole moment. Myers (*93*) has utilized the differences in I^{127} line widths in I^-, I_2, and I_3^- to study the kinetics of triiodide formation.

$$I^- + I_2 \underset{k_2}{\overset{k_1}{\rightleftharpoons}} I_3^- \tag{37}$$

In aqueous iodide solution to which small amounts of iodine has been added, the I^{127} resonance for I^- is broadened over that for pure iodide solutions. Degree of broadening here is related to the average lifetime of an iodine nucleus as I_3^-. These experimental conditions then appear to meet the conditions of slow exchange. The frequency separations between the I^- and I_2 and between the I^- and I_3^- resonances are not known, but presumably these are large with respect to the I^- line width and Eq. (38) is valid for this system.

$$1/T_{2A}' = 1/T_{2A} + 1/\tau_{I^-} \tag{38}$$

Analysis of line width variation with respect to initial I^- and I_2 concentrations gave values of

$$k_1 = 4.1 \pm 0.4 \times 10^{10} \text{ 1/sec}^{-1}\ M^{-1}$$

$$k_2 = 7.6 \pm 0.8 \times 10^{7} \text{ sec}^{-1}$$

These extraordinarily fast reactions probably are not kinetically analyzable by alternative techniques. Opportunities for studies of similar, fast solution reactions by NMR appear unlimited.

F. Exchange in Paramagnetic Systems

Formally similar to NMR kinetic analysis of systems in which nuclei are subject to quadrupolar relaxation effects are systems which are influenced by paramagnetic species. Interaction of a magnetic nucleus with a paramagnetic molecule or ion leads to a decrease in the longitudinal (T_1) and transverse (T_2) relaxation times of the nucleus. An example of this is found in the proton resonance of aqueous solutions of transition metal ions. For many ions, the most important relaxation mechanism is an electron-nucleus dipole-dipole interaction. In these cases, nuclear T_1's and T_2's are approximately equal and show a linear dependence on the reciprocal concentration of paramagnetic ion. For paramagnetic ions that have long electron relaxation times [long enough to observe a relatively sharp electron paramagnetic resonance (EPR) signal] another mechanism, an exchange interaction, contributes to the transverse relaxation time and leads to very small T_2 values (*118*). This mechanism, as developed by Bloembergen and Morgan (*8*), is a scalar coupling, $\mathbf{AI \cdot S}$, between the nuclear spin of the proton and the electron spin of the paramagnetic ion. This relaxation mechanism has a common origin with the isotropic hyperfine contact interaction shifts discussed in Section V (p. 280). This formulation has been verified by studies of manganous ion solutions (*5*), and the temperature dependence of T_2 and T_1 has been utilized to derive values for proton exchange between solvent water and water in the coordination sphere of the manganous ion ($Mn(H_2O)_6^{++}$).

For the complete expressions for T_1 and T_2 the reader is referred to the original literature (*5*). Let it suffice here to note that the temperature dependent term resides in the correlation times τ_c (dipolar interaction) and τ_e (exchange interaction). The temperature dependences of the individual correlation times are:

$$\begin{aligned} \tau_c &= \tau_c^0 \exp (V_c/RT) \\ \tau_h &= \tau_h^0 \exp (V_h/RT) \\ \tau_s &= \tau_s^0(T - T^0)/T^0 \end{aligned} \tag{39}$$

where V_c is the activation energy for the molecular motion of the hydrated ion (approximately equal to that for the rotation of the hydrated ion) and V_h is the activation energy for proton exchange over the temperature range T to T^0. Because proton exchange can destroy the scalar coupling, the lifetime, τ_h, of a proton in the hydration sphere of Mn^{++}, in addition

to the electron correlation time, τ_s, contributes to the over-all exchange correlation time τ_e, i.e.,

$$1/\tau_e = 1/\tau_h + 1/\tau_s. \tag{40}$$

Substitution of Eqs. (39) into Eq. (40) gives the temperature dependence of the net correlation time

$$1/\tau_e = \frac{\exp(-V_h/RT)}{\tau_h^0} + \frac{T^0}{\tau_s^0(T - T^0)} \tag{41}$$

In Fig. 18, the experimental dependence of T_2 on temperature in a manganous ion solution is presented and compared with the theoretical relation. Agreement is good and these data permit an evaluation of the

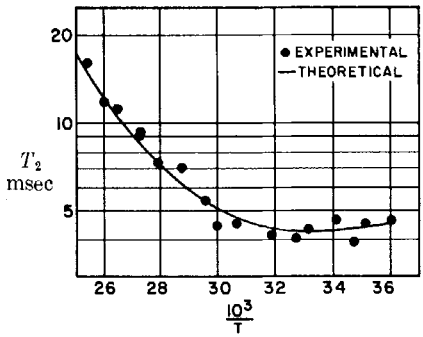

FIG. 18. Experimental and theoretical curves for dependence of the transverse relaxation time T_2 on temperature for protons in an aqueous solution of manganous ion at a resonance frequency of 10 Mc/sec. [Bernheim *et al.* (*5*).]

proton lifetime in the hydration sphere. Since the dipolar contributions to T_1 and T_2 are essentially identical, the exchange contributions to T_2 can be calculated:

$$(1/T_2)_{exch.} = (1/T_2)_{obsd.} - (1/T_2)_{dipolar} = (1/T_2)_{obsd.} - (1/T_1)_{dipolar}. \tag{42}$$

Contributions to $(T_2)_{exch.}$ include effects of τ_h and τ_s. A plot of log $[(T_2)_{exch.} - C/\tau_s]$* vs. 1/T gives 8.4 kcal/mole for the activation energy of proton exchange between water and the hydration sphere of the manganous ion. For more recent data on exchange involving $Mn(H_2O)_6^{++}$, the interested reader is directed to the O^{17} NMR studies of Connick and Swift (*16a*).

G. Electron Exchange

McConnell and Weaver (*78*) have utilized line width measurements of Cu^{63} and Cu^{65} resonances in a Cu^{I}—Cu^{II}—HCl system to estimate the

* C is a constant evaluated under conditions of slow exchange.

rate of electron exchange between Cu^{I} and Cu^{II}. Experimentally, it is found that the Cu^{63} resonance of $1M$ [CuCl] in concentrated hydrochloric acid is progressively broadened with addition of copper(II) chloride. The broadening here is due to a relaxation mechanism associated with the Cu^{I}—Cu^{II} electron exchange. Eq. (32) is applicable here and in this case T'_{2A} is the observed transverse nuclear relaxation time for a Cu^{I}—Cu^{II} system, T_{2A} is the transverse nuclear relaxation time for the pure Cu^{I} system and τ_A is the lifetime of a Cu^{I} state. With the assumption that the electron transfer process follows a bimolecular rate law, it follows that

$$\tau_{A_{Cu^{I}}} = [1/k(Cu^{II})] \tag{43}$$

and

$$\tau_{A_{Cu^{II}}} = [1/k(Cu^{I})]. \tag{44}$$

Accordingly, evaluation of k from line-width measurements gives a bimolecular rate constant of 0.5×10^8 l sec^{-1} M^{-1}. This is one of the fastest electron exchange reactions studied in aqueous solution. Transfer rate here may not describe direct electron transfer between Cu^{I} and Cu^{II}; Stranks has suggested (*129*) that the rate may refer to transfer within a bridged activated complex, e.g.,

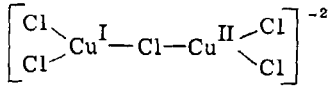

Unquestionably, extensive future use will be made of NMR in the important problem of understanding electron exchange processes in metal complexes. There are many nuclei within the transition group that are probably suitable for such studies, e.g., V^{51}, Mn^{55}, Co^{59}, Nb^{93}, and Mo^{95}. A recent application (*36*) has dealt with electron exchange between V^{IV} and V^{V} in acid chloride solutions.

V. Hyperfine Contact Interaction Shifts

A. Paramagnetic Chelates and Organometallics

In paramagnetic systems an interaction can exist between unpaired electrons and nuclei possessing magnetic moments which is of the form $\mathbf{I}\cdot\mathbf{S}$. In the hydrogen atom, for example, this interaction is manifested in the EPR spectrum by the appearance of a doublet of spacing 508 gauss. The origin of the doublet is the Fermi contact interaction which is given by the expression (*29*)

$$a = \frac{8\pi}{3h} g_e g_H \beta_e \beta_H [\psi(0)]^2 \tag{45}$$

where a is the contact interaction constant, g_e and g_H are respectively the electron and proton "g-values," β_e and β_H are respectively the Bohr magneton and nuclear magneton and $\psi(0)$ is the value of the wave function describing the distribution of the unpaired electron evaluated at the nucleus. This Fermi contact interaction is manifested in the electron paramagnetic resonance spectra of radical species as the hyperfine structure. For example, in the benzene negative ion a seven line hyperfine structure is observed of spacing 22.5/6 gauss (*134*). Observation and analysis of hyperfine splittings has become an important approach to the elucidation of the electronic structures of molecules.

McConnell (*74*) has shown that for the case of aromatic radical species where the interaction is between a spin density localized on a $p\pi$ orbital of a carbon atom and the proton bonded to that carbon atom a relationship exists between an observed proton contact interaction constant a_i and the spin density ρ_i on the adjacent carbon atom. This relationship is

$$a_i \cong Q\rho_i \tag{46}$$

where Q is a proportionality constant characteristic of the particular mechanism giving rise to the **I·S** interaction. Q for an aromatic ·C—H fragment is -22.5 gauss (*134*) and for a ·C—CH_3 fragment, the best current value is about $+27$ gauss (*31*). For a ·C—CH_3 fragment, the CH_3 protons "sense" the spin density on the $p\pi$ orbital of the adjacent carbon atom directly by a hyperconjugation mechanism and so the sign of Q is positive. For the aromatic ·C—H fragment, however, only an indirect sensing mechanism (involving an interaction between π- and σ-electrons) is possible and so the sign of Q here is negative. Signs of Q and ρ are not determinable from the EPR experiment; however, as we shall see, signs of ρ in paramagnetic systems are manifested in an NMR experiment by the direction of resonance field shift.

At this point it would be well to differentiate clearly between *spin* densities, ρ's, which are obtained experimentally from contact interaction constants, and *electron* densities in molecules. If a simple Hückel LCAO MO calculation is carried out on the allyl radical, the computed distribution of the single unpaired electron is as shown below

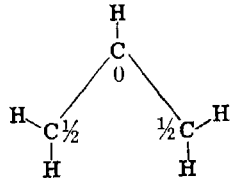

The valence bond calculation as carried out on the allyl radical, however, gives the spin density distribution (*75*)

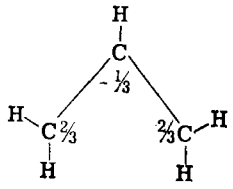

An experimental determination of the spin density distribution in the allyl radical recently has become available (*30*) and is in fair agreement with the results of the valence bond calculation and in somewhat better agreement with an extended Hartree-Fock calculation to be described below. It is seen that although the allyl radical possesses only a single unpaired electron, the total calculated π-electron spin density on the molecule is $\frac{5}{3}$ to $\frac{3}{2}$ units depending on the approximation employed. However, the relationship (*75*)

$$\sum_{i=1}^{3} \rho_i = 1 \tag{47}$$

is obeyed.

The origin of total molecular spin densities greater than one for doublet state radicals is most clearly shown by an extended Hartree-Fock calculation on the allyl radical carried out by MacLachlan (*79*). The distributions of the three π-electrons of the allyl radical are by this calculation those shown below.

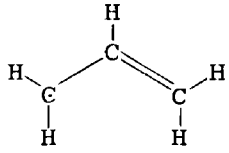

$\psi_0^2\ (\alpha)$	0.50	0	0.50
$\psi_1^2\ (\alpha)$	0.31	0.38	0.31
$\psi_1^2\ (\beta)$	-0.19	-0.62	-0.19

In both the extended Hartree-Fock calculation and the valence bond calculation effects of spin correlation are included, but not in the simple Hückel scheme. The π-energy levels for the allyl radical are shown schematically below.

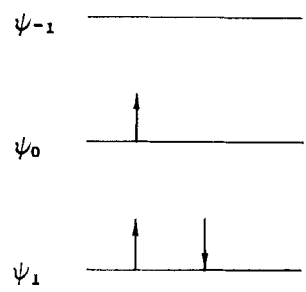

We see in the extended Hartree-Fock calculation where effects of spin correlation are included that the two electrons of α- and β-spin in the orbital designated ψ_1 are distributed differently. This can be thought of as a polarization effect in which there is an exchange interaction between the electron of α-spin in ψ_0 and the electron of α-spin in ψ_1. This polarization results in a migration of the electron of α-spin in ψ_1 away from the central carbon atom of the allyl radical leaving a net β or negative spin density at this carbon atom. Signs cannot be distinguished in the EPR experiment; negative spin densities are manifested by hyperfine splittings in precisely the same fashion as are positive spin densities. It will be seen below that signs of spin densities can, however, be determined in the NMR experiment in paramagnetic systems to which the technique is applicable. It should be pointed out that the sign of the spin density is an important parameter. In alternate radical systems, spin densities are all positive whereas in odd alternate systems the signs of spin densities are alternately + and −. The sequences of spin density signs in a conjugated paramagnetic system can be revealing as to the mechanism of the propagation of conjugation effects.

Normally one cannot observe in paramagnetic systems the characteristic chemical shifts and nuclear spin-spin splittings which make high resolution NMR so valuable in chemical and physical applications. This is because the presence of the electronic paramagnetism gives rise to an electron-nucleus relaxation mechanism which tends to broaden the resonances to the point where only a single, broad signal is observable. It has been pointed out (*75*) however, that if either or both of two conditions exist in a paramagnetic system,

$$T_1^{-1} \gg a_i$$
$$T_e^{-1} \gg a_i$$

isotropic hyperfine contact interaction shifts are superimposed on the chemical shifts. In the above inequalities T_1 is the electron relaxation time of the paramagnetic system and T_e is the characteristic exchange time. If either or both of these conditions are satisfied in a paramagnetic system, the

nuclei experience a time-averaged isotropic contact hyperfine interaction field which is given by (*76*, *77*)

$$\left(\frac{\Delta H}{H}\right)_i = a\frac{\gamma_e}{\gamma_N}\langle S_z\rangle_{av}, \tag{48}$$

where

$$\langle S_z\rangle_{av} = \frac{\sum_i S_i e^{-(E_i/kT)}}{\sum_i e^{-(E_i/kT)}} \tag{49}$$

S is the electron spin quantum number and $E_i = g\beta S_i H$. Nuclear resonance field shifts ΔH then are observed which are given by the expression

$$\left(\frac{\Delta H}{H}\right)_i = -a_i\frac{\gamma_e}{\gamma_N}\frac{g\beta S(S+1)}{3kT} \tag{50}$$

where H is the nuclear resonance field and γ_e and γ_N are respectively the magnetogyric ratios of the electron and the nucleus under observation. Thus, in favorable situations the contact interaction constants a_i of a paramagnetic system can be derived from measurements of the NMR contact interaction shifts, $(\Delta H/H)_i$.

Rather extensive studies of contact interaction shifts have been carried out on the nickel(II) chelates of the substituted aminotroponeimineates (*4*, *103*). The H^1 spectrum of the nickel(II) chelate of 1-(2-naphthylamino)-7-(2-naphthylimino)-1,3,5-cycloheptatriene in $CDCl_3$ is shown in Fig. 19. There are ten nonequivalent sets of protons in this chelate and the same number of proton resonances are observed. Resonances designated α, β, and γ can be assigned to the three nonequivalent sets of protons of the seven-membered ring. The seven resonances of the β-naphthyl group are shown expanded in Fig. 20. The total spread of these seven proton resonances in the nickel(II) chelate is about 1800 cps (at 60 Mc/sec and 23°C) and for the diamagnetic zinc chelate about 50 cps. The positions of the proton resonances of the zinc chelate are indicated by the zero on the base line of Fig. 20. It is seen that four of the β-naphthyl resonances in the nickel(II) chelate are shifted to high field and three to low field. High field contact shifts for aromatic C—H fragments indicate positive carbon atom spin densities, and low field shifts indicate negative carbon atom spin densities. The N-substituted aminotroponeimineate ligand is nonalternate so on the β-naphthyl group we expect an alternating sequence of spin density signs. Four of the seven H^1 resonances of the β-naphthyl group exhibit resolvable nuclear spin-spin structure (two doublets indicating that these protons are immediately flanked by only one other proton and two triplets indicating protons with two adjacent hydrogen atoms).

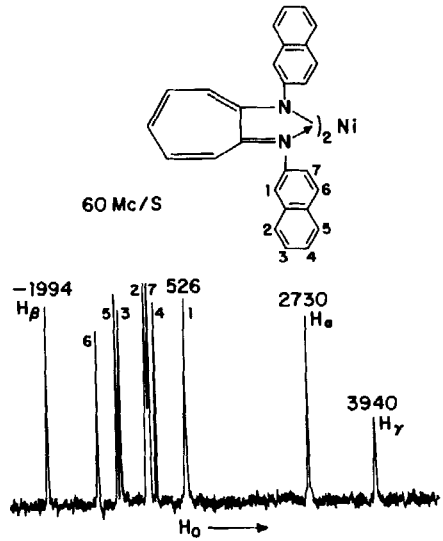

FIG. 19. H^1 spectrum of the nickel(II) chelate of 1-(2-naphthylamino)-7-(2-naphthylimino)-1,3,5-cycloheptatriene in $CDCl_3$. [Benson *et al.* (*4*).]

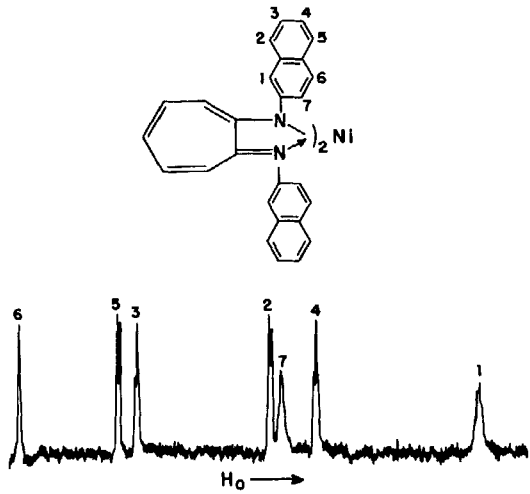

FIG. 20. Expanded H^1 spectrum of the β-naphthyl protons of the nickel(II) chelate of 1-(2-naphthylamino)-7-(2-naphthylimino)-1,3,5-cycloheptatriene. [Benson, Eaton, Josey, and Phillips (*4*).]

Assignments were made on the basis of the above considerations. Using Eq. (50) and the measured susceptibility, the observed spin density distribution for the β-naphthyl chelate is shown in Fig. 21. All spin densities in these chelates arise, of course, from the two unpaired electrons of nickel(II)

in the d^8 configuration. Spin density is introduced *onto* the π-system of the ligand as a result of metal-ligand bonding. In most cases it is not clear whether spin densities are introduced onto ligands as a result of direct delocalization of the unpaired $3d$ electrons of the transition metal or through spin polarization effects not involving direct delocalization. However, measurements of this kind should be of value in furnishing new insights into the important and still obscure problem of the nature of bonding in chelates and organometallics.

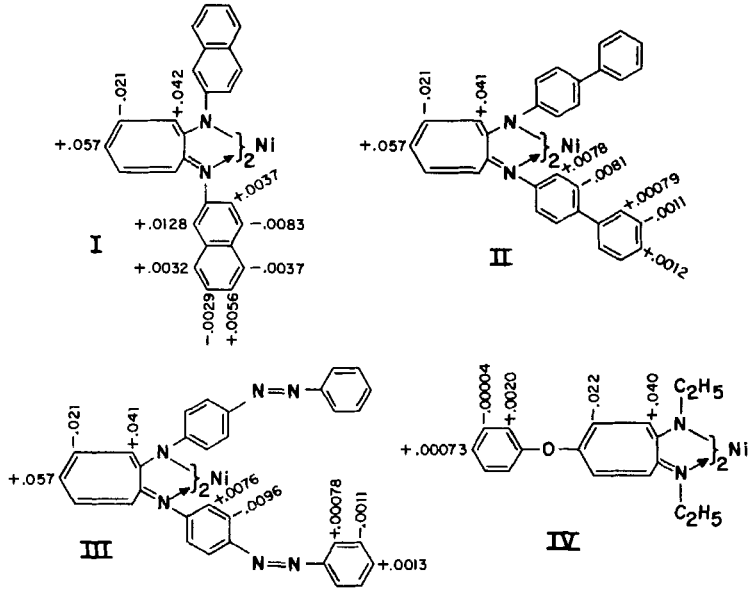

FIG. 21. Spin density distribution in some nickel(II) aminotroponeimineates. [Benson *et al.* (4).]

Irrespective of the nature of metal-ligand bonding, contact shifts in paramagnetic chelates can be employed to map spin density distributions in conjugated ligands and generally elucidate conjugation effects in molecules. An important point to be recognized is that in these systems spin densities are introduced onto the ligand atoms directly bonded to the metal atoms. These spin densities then are distributed throughout the conjugated system in a fashion that is determined primarily by the electronic structure of the ligand's π-system. Thus, for example, in II and III of Fig. 21 we see that spin densities on the second phenyl rings of the biphenyl- (II) and azobenzene- (III) substituted nickel aminotroponeimineates are less than those of the first ring. From this comparison we see too that the azo linkage is highly effective in transmitting spin densities. Such quantitative measure-

ment of attenuation of conjugative effects in π-systems currently is of importance in the understanding of the effects of conjugated ligands in enhancing rates of electron exchange in systems where chelates are involved.

In IV of Fig. 21 is seen that spin density is transmitted through the oxygen atom linking the phenyl and seven-membered ring. In the valence bond formulation, the only way spin density can be transferred from the seven-ring to the phenyl ring is through contributions of ionic structures such as

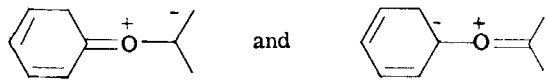

to the ground electronic state of the molecule. It is noteworthy that structures of the same form are required in the superexchange mechanisms of Kramers (*63*) and Anderson (*1*) to account for the ferromagnetic and antiferromagnetic ordering of spins in magnetic transition metal oxides and sulfides.

B. Magnetic Interactions in Solids

Tinkham (*130*) first observed additional splittings in the EPR spectrum of Mn^{++} embedded in an ZnF_2 lattice that could only be attributed to an interaction between the 3*d*-electrons of Mn^{++} and the surrounding fluorine nuclei. It was postulated that the Mn^{++}—F^- bonds are not purely ionic and that the unpaired electrons have finite probability densities on the fluorine orbitals. In other words, the Mn^{++}—F^- bonds are partially covalent in character. These conclusions derived from EPR hyperfine splittings were confirmed by Shulman and Jaccarino (*126*) when they observed a shift in the F^{19} spectrum of solid MnF_2. Such a shift would be expected in the F^{19} spectrum if covalent or charge transfer structures such as Mn^+—F^0 contributed to the electronic structure of the system. Shulman (*125*) also has observed a shift in the N^{14} spectrum of $Fe(CN)_6^{2-}$ which is at least partially attributable to a finite probability density of the unpaired electrons of the ferric ion residing at the nitrogen atoms of the cyano groups. Important results of the electronic structures of complexes and chelates of the transition and rare earth elements will be forthcoming from other studies of this nature.

VI. NMR of Solids

The NMR observables of a substance as a liquid, solution, or in the gas phase of paramount importance to the inorganic chemist are chemical shifts and nuclear spin-spin coupling constants. In the solid state, however, these effects generally are dwarfed by anisotropic dipolar interactions so

that chemical shifts and coupling constants experimentally are not observable, and one usually is confronted with analysis of a single, structureless absorption peak with a width of up to tens of gauss. Application of NMR to inorganic solids has given a great deal of new information concerning structures of molecules and ions, phase transformations, diffusion in solids, electronic structures of conductors and semiconductors, and magnetic interactions and spin structure in ferromagnetic and antiferromagnetic substances. Such information is of interest not only to physicists and physical chemists but also to those working in the rapidly developing new field of solid state inorganic chemistry.

Consider two nuclei A and B which possess nuclear moments μ_A and μ_B, separated by a distance r_{AB} and which are subjected to a magnetic field H_0 whose direction defines the z-axis. Then if $\mu_A = \mu_B$, a quantum mechani-

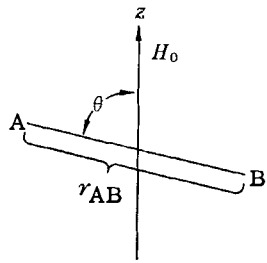

cal perturbation calculation (*100*) shows that a field in the z-direction is produced at A by μ_B which is given by

$$(H_{loc})_z = \frac{3}{2} \cdot \frac{\mu}{r_{AB}^3} (3 \cos^2 \theta - 1). \tag{51}$$

Since there is a reciprocal effect of μ_A on B, a doublet resonance is expected with spacing

$$\frac{3\mu}{r_{AB}^3} (3 \cos^2 \theta - 1).$$

Note that the above model refers to a single crystal containing only two interacting like nuclei and is a good first approximation to, for example, a hydrate where because of the r_{AB}^{-3} dependence of the dipolar interaction, the two protons of a given H_2O molecule provide the dominant interaction. Interactions between protons on different H_2O molecules serve mainly as a source of line broadening. The first example of such an application was by Pake on single crystals of gypsum (*100*). Gypsum has the formula $CaSO_4 \cdot 2H_2O$ and contains two differently oriented water molecules per unit cell. From a detailed analysis of the resonance line shape as a function

of crystal orientation, Pake deduced an intermolecular proton-proton separation of 1.58 A for the water molecules.

More often than not, one is forced to study a polycrystalline sample rather than a single crystal. If as above the dominant dipolar interaction is between two identical nuclei with $I = \frac{1}{2}$, a doublet resonance is observed of spacing $3r_{AB}^{-3}$. Studies on powders have, for example been useful in elucidating the nature of the H—F bond in $[FHF]^-$ (*137*) and in establishing the existence of the H_3O^+ ion in solid $HNO_3 \cdot H_2O$ (*117*). For this latter study the calculated line shape for three interacting nuclei at the vertices of an equilateral triangle was shown to be in agreement with experiment. However, line shape calculations on more complicated systems become tedious and instead the van Vleck treatment of second moments (*135*) generally is used to obtain information about internuclear distances from NMR studies on solids.

Perhaps a more generally useful application of NMR to solids derives from the sensitivity of NMR line widths and shapes to inter- and intramolecular motion. The angular term $(3 \cos^2 \theta - 1)$ that appears in the expression for the nuclear dipole-dipole interaction as for example in Eq. (51) can be either partially or completely averaged by rotational or translational motions in the solid. Motional narrowing effects on resonances are observed when the characteristic frequency of the motion becomes comparable with the resonance line width expressed in frequency units, i.e., about 10^4 to 10^6 sec^{-1}. Thus in the rigid lattice at low temperatures where all inter- and intramolecular motions are "frozen out," the maximum NMR line width is observed. Upon increasing the temperature, line width decreases are observed as the various first and second order transitions possible to the solid are passed through. Finally at the melting point the $(3 \cos^2 \theta - 1)$ term is completely averaged (at least for low viscosity liquids) and chemical shifts and nuclear spin-spin interaction again become observable in the NMR spectra.

A particularly interesting example of the effect of molecular motions on NMR line widths was observed by Murray and Waugh for $Co(NH_3)_6Cl_3$ (*92*). Theoretical line shapes for the proton resonance of $Co(NH_3)_6Cl_3$ are shown in Fig. 22 for (1) a rigid lattice, (2) rotation about the Co—N bond, and (3) rotation of the entire $Co(NH_3)_6^{3+}$ ion in the crystal lattice. Experimental points for H^1 spectra at 100°K and 300°K are seen to fall quite well on curves calculated for, respectively, models (2) and (3). Thus even at 100°K rotation about the Co—N bond at frequencies in excess of about 10^4 sec^{-1} is occurring. Between 100°K and 300°K, the frequency of rotation of the $Co(NH_3)_6^{3+}$ ion exceeds 10^4 sec^{-1}.

There are a number of areas where NMR has made significant contributions that are of more interest to the solid state inorganic chemist than to the molecular inorganic chemist. These applications will not be treated here

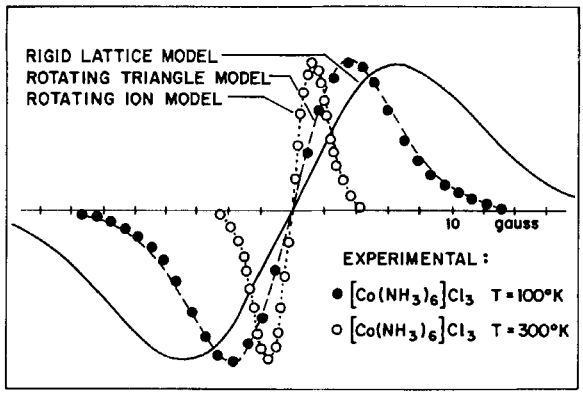

FIG. 22. Theoretical and experimental proton line shape derivatives in solid $Co(NH_3)_6Cl_3$. [Murray and Waugh (*92*).]

in any detail because they generally depend on rather extensive theoretical developments. Rather, some of these applications will be mentioned and the reader is referred to the original literature for more detailed treatment. It is to be expected that it will be in these areas that the NMR of solids will make its most important future contributions.

Symmetries of local electrical environments of quadrupolar nuclei ($I \geqslant 1$) profoundly influence relaxation times and resonance line shapes of such nuclei (*9*, *116*). Consider a nucleus for which $I = \frac{3}{2}$ (Br^{79}, B^{11}). In the absence of quadrupolar perturbation, the nuclear spin levels are evenly spaced, as shown in I below, and the three possible nuclear resonance transitions have equal energies ($\Delta m = \pm 1$). If, however, $eqQ \neq 0$

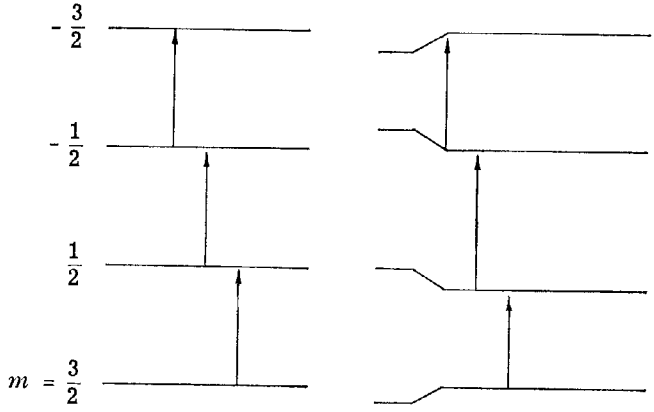

the four levels are displaced and three transitions of different energies become possible. A higher order effect will also displace the $\frac{1}{2} \rightarrow -\frac{1}{2}$ transition. Reif in an important study (*116*) has utilized such effects on bromine resonances to investigate diffusion and imperfections in AgBr lattices. Recently Silver and Bray have studied (*127*) the second order displacements of the $\frac{1}{2} \rightarrow -\frac{1}{2}$ resonance of B^{11} to obtain boron quadrupole coupling constants in B_2O_3 and some sodium borate glasses. From the electrical symmetries about boron, deduced from the quadrupole coupling constants, it was possible to draw some conclusions about the structures of these materials.

It was found by Knight in 1949 (*62*) that nuclear resonances of elements as metals were displaced to low field (at constant frequency) from the resonances of the elements as salts. These large shifts ($\Delta H/H_0 = 0.1\%$ to 1%), called Knight shifts, were attributed to interaction between the nuclei and electrons near the top of the Fermi distribution polarized by the magnetic field. These electrons, the conduction electrons, often have a large probability distribution near the nuclei and can be thought of as producing large local internal fields at the nuclei. The expression for the Knight shift is (*133*)

$$\frac{\Delta H}{H_0} = \frac{a\chi_p M\langle|\psi_F(0)|^2\rangle_{av}}{2\gamma\hbar\beta|\psi_A(0)|^2} \tag{52}$$

where a is the Fermi contact interaction constant defined by Eq. (45), χ_p is the electron spin susceptibility of electrons in the conduction band, M is the nuclear mass and $\langle|\psi_F(0)|^2\rangle_{av}$ is the probability density at the nucleus of all electronic states on the Fermi surface. The close similarity between the Knight shift [Eq. (52)] and the contact interaction shift discussed earlier [Eq. (50)] is apparent. The Knight shift, through the factor $\langle|\psi_F(0)|^2\rangle_{av}$, has provided a sensitive tool for testing wave functions developed to describe the behavior of conduction electrons in metals.

Knight shifts produced by the conduction electrons of metals are generally somewhat greater than the chemical shifts of nuclei in different molecular environments. However, both of these shifts are small compared to the external fields generally employed for observation of NMR (1000–15,000 gauss). In ferromagnetic and antiferromagnetic substances below, respectively, the Curie and Néel temperatures, internal fields resulting from spin alignment in the magnetic state can be very much greater than conveniently accessible laboratory fields. For example, the Co^{59} resonance in ferromagnetic face-centered cobalt occurs at 213 Mc/sec in zero applied field at 300°K (*36a*). From Eq. (6) and the known magnetogyric ratio for Co^{59} this frequency corresponds to a resonance field of 213,400 gauss. Similarly in ferromagnetic iron, the Fe^{57} resonance frequency of 45 Mc/sec corresponds to a local internal field of 330,000 gauss (*36b*).

Above the Curie and Nèel temperatures, ferromagnetic and antiferromagnetic substances behave as simple paramagnetic substances without long range electron spin correlation, and "normal" nuclear resonances are observed. The electron moments produce effects on the nuclei that are small because of averaging over the distribution of states available to the electron spins. However, below these magnetic transition temperatures, spins are aligned throughout the solid to varying degrees of sublattice complexity and the nuclei consequently "see" huge local fields. Studies of ferromagnetic and antiferromagnetic resonances are quite new but it is very apparent even at this early date that they will be valuable in elucidating the mysteries of magnetic interactions in solids.

References

1. Anderson, P. W., *Phys. Rev.* **79,** 350 (1950).
2. Anderson, P. W., *J. Phys. Soc. Japan* **9,** 316 (1954).
3. Andrew, E. R., Bradbury, A., Eades, R. G., and Jenks, G. F., *Nature* **188,** 1097 (1960).
4. Benson, R. E., Eaton, D. R., Josey, A., and Phillips, W. D., *J. Am. Chem. Soc.*, **83,** 3714 (1961).
5. Bernheim, R. A., Brown, T. H., Gutowsky, H. S., and Woessner, D. E., *J. Chem. Phys.* **30,** 950 (1959).
6. Berry, S., *J. Chem. Phys.* **32,** 933 (1960).
7. Bloch, F., Hansen, W. W., and Packard, M. E., *Phys. Rev.* **69,** 127 (1946).
8. Bloembergen, N., and Morgan, L. O., *J. Chem. Phys.* **34,** 842 (1961).
9. Bloembergen, N., Purcell, E. M., and Pound, R. V., *Phys. Rev.* **73,** 679 (1948).
10. Bothner-By, A. A., and Naar-Colin, C., *J. Am. Chem. Soc.* **80,** 1728 (1958).
11. Bothner-By, A. A., and Naar-Colin, C., *Ann. N. Y. Acad. Sci.* **70,** 833 (1958).
11a. Bramley, R., Figgis, B. N., and Nyholm, R. S., private communication to E. L. Muetterties (1961).
12. Braune, H., and Pinnow, P., *Z. physik. Chem. (Leipzig)* **B35,** 239 (1937).
13. Brockway, L. O., and Beach, J. Y., *J. Am. Chem. Soc.* **60,** 1836 (1938).
14. Burke, J. J., and Lauterbur, P. C., *J. Am. Chem. Soc.* **83,** 326 (1961).
15. Cady, G. H., and Shreeve, J. M., private communication to E. L. Muetterties (1961).
15a. Clark, H. C., private communication to E. L. Muetterties (1961).
16. Cleaver, C. S., and Phillips, W. D., unpublished results.
16a. Connick, R. E., and Swift, T., "Advances in the Chemistry of the Coordination Compounds," p. 15. Macmillan, New York, 1961.
16b. Connick, R. E., and Stover, E. D., *J. Phys. Chem.* **65,** 2075 (1961).
17. Connor, T. M., and Loewenstein, A., *J. Am. Chem. Soc.* **83,** 560 (1961).
17a. Corio, P. L., *Chem. Rev.* **60,** 363 (1960).
17b. Cotton, F. A., Danti, A., Waugh, J. S., and Fessenden, R. W., *J. Chem. Phys.* **29,** 1427 (1958).
18. Cotton, F. A., George, J. W., and Waugh, J. S., *J. Chem. Phys.* **28,** 994 (1958).
19. Coulson, C. A., and Longuet-Higgins, H. C., *Proc. Roy. Soc.* **A191,** 39 (1947).
20. Coyle, T. D., and Stone, F. G. A., *J. Chem. Phys.* **32,** 1892 (1960).
21. Dailey, B. P., and Shoolery, J. N., *J. Am. Chem. Soc.* **77,** 3977 (1955).
22. Das, T. P., *J. Chem. Phys.* **27,** 1 (1957).
23. Dehm, H. C., and Chien, J. C. W., *J. Am. Chem. Soc.* **82,** 4429 (1960).

23a. Dharmatti, S. S., and Weaver, H. E., *Phys. Rev.* **87,** 675 (1952).
24. Dickinson, W. C., *Phys. Rev.* **80,** 563 (1950).
25. Diehl, P., and Ogg, R. A., Jr., *Nature* **180,** 1114 (1957).
26. Dodd, R. E., Woodward, L. A., and Roberts, H. L., *Trans. Faraday Soc.* **52,** 1052 (1955).
26a. Dreitlein, J., and Kessemeier, H., *J. Chem. Phys.* **123,** 835 (1961).
26b. Eaton, D. R., and Sheppard, W. A., unpublished data.
27. Emerson, M. T., Grunwald, E., and Kromhout, R. A., *J. Chem. Phys.* **33,** 547 (1960).
28. Ettinger, R., Johnson, F. A., and Colburn, C. B., *J. Chem. Phys.* **34,** 2187 (1961).
29. Fermi, E., *Z. Physik* **60,** 320 (1930).
30. Fessenden, R. W., private communication to W. D. Phillips (1961).
31. Fessenden, R. W., and Schuler, R. H., *J. Chem. Phys.* **33,** 935 (1960).
32. Fraenkel, G., Carter, R. E., McLachlan, A. D., and Richards, J. H., *J. Am. Chem. Soc.* **82,** 5846 (1960).
33. Frank, P. J., and Gutowsky, H. S., *Arch. sci.* (*Geneva*) **11,** 215 (1958).
34. Freeman, R., Gasser, R. P. H., and Richards, R. E., *Mol. Phys.* **2,** 301 (1959).
35. Freeman, R., Murray, G. R., and Richards, R. E., *Proc. Roy. Soc.* **A242,** 455 (1957).
36. Giuliano, C. R., and McConnell, H. M., *J. Inorg. & Nuclear Chem.* **9,** 171 (1959).
36a. Gossard, A. C., and Portis, A. M., *Phys. Rev. Letters* **3,** 164 (1959).
36b. Gossard, A. C., and Portis, A. M., *J. Phys. Chem. Solids* **17,** 341 (1961).
37. Green, M. H. L., Pratt, L., and Wilkinson, G., *J. Chem. Soc.* p. 3916 (1958).
38. Green, M. H. L., McCleverty, J. A., Pratt, L., and Wilkinson, G., *J. Chem. Soc.* p. 4854 (1961).
39. Griffith, J. S., and Orgel, L. E., *Trans. Faraday Soc.* **53,** 601 (1957).
40. Griffith, W. P., and Wilkinson, G., *J. Chem. Soc.* p. 2757 (1959).
41. Grunwald, E., Karabatsos, P. J., Kromhout, R. A., and Purlee, E. L., *J. Chem. Phys.* **33,** 556 (1960).
42. Grunwald, E., Loewenstein, A., and Meiboom, S., *J. Chem. Phys.* **27,** 630 (1957).
43. Grunwald, E., Loewenstein, A., and Meiboom, S., *J. Chem. Phys.* **25,** 382 (1956).
44. Gutowsky, H. S., and Holm, C. H., *J. Chem. Phys.* **25,** 1228 (1956).
45. Gutowsky, H. S., Karplus, M., and Grant, D. M., *J. Chem. Phys.* **31,** 1278 (1959).
46. Gutowsky, H. S., and McCall, D. W., *Phys. Rev.* **82,** 748 (1951).
47. Gutowsky, H. S., McCall, D. W., and Slichter, C. P., *J. Chem. Phys.* **21,** 279 (1953).
48. Hahn, E. L., and Maxwell, D. E., *Phys. Rev.* **84,** 1246 (1951).
49. Hamer, A. N., *J. Inorg. & Nuclear Chem.* **9,** 98 (1959).
50. Harrison, B. C., Solomon, I. J., Hites, R. D., and Klein, M. J., *J. Inorg. & Nuclear Chem.* **14,** 195 (1960).
51. Hecht, H. C., Grant, D. M., and Eyring, H., *Mol. Phys.* **3,** 577 (1960).
52. Heck, R. F., and Breslow, D. S., *J. Am. Chem. Soc.* **82,** 750 (1960).
53. Hoffmann, C. A., Holder, B. E., and Jolly, W. L., *J. Phys. Chem.* **62,** 364 (1958).
54. Jackson, J. A., Lemons, J. F., and Taube, H., *J. Chem. Phys.* **32,** 553 (1960).
55. James, H. M., and Coolidge, A. S., *J. Chem. Phys.* **1,** 825 (1933).
56. Johnson, C. E., and Bovey, F. A., *J. Chem. Phys.* **29,** 1012 (1958).
57. Jonassen, H. B., Stearns, R. I., Kenttämaa, J., Moore, D. W., and Whittaker, A. G., *J. Am. Chem. Soc.* **80,** 2586 (1958).
58. Jones, D., Parshall, G. W., Pratt, L., and Wilkinson, G., *Tetrahedron Letters*, p. 48 (1961).
59. Karplus, M., *J. Chem. Phys.* **30,** 11 (1959).

60. Karplus, M., Anderson, D. H., Farrar, T. C., and Gutowsky, H. S., *J. Chem. Phys.* **27,** 597 (1957).
61. Karplus, M., and Grant, D. M., *Proc. Natl. Acad. Sci. U. S.* **45,** 1269 (1959).
62. Knight, W. D., *Phys. Rev.* **76,** 1259 (1949).
63. Kramers, H., *Physica* **1,** 182 (1930).
64. Kubo, R., *J. Phys. Soc. Japan* **9,** 935 (1954).
65. Lamb, W. E., *Phys. Rev.* **60,** 817 (1941).
66. Lauterbur, P. C., "Determination of Structures of Organic Molecules," Chapter 7. Academic Press, New York, 1962.
67. Lipscomb, W. N., *Advances in Inorg. Chem. and Radiochem.* **1,** 132 (1959).
68. Loewenstein, A., and Meiboom, S., *J. Chem. Phys.* **27,** 1067 (1957).
69. McClellan, W. R., Hoehn, H. H., Cripps, H. N., Muetterties, E. L., and Howk, B. W., *J. Am. Chem. Soc.* **83,** 1601 (1961).
70. McCleverty, J. A., and Wilkinson, G., *Chem. & Ind. (London)* p. 288 (1961).
71. McConnell, H. M., *J. Chem. Phys.* **24,** 460 (1956).
72. McConnell, H. M., *J. Chem. Phys.* **27,** 226 (1957).
73. McConnell, H. M., *J. Chem. Phys.* **28,** 430 (1958).
74. McConnell, H. M., *Proc. Natl. Acad. Sci. U. S.* **43,** 721 (1957).
75. McConnell, H. M., and Chesnut, D. B., *J. Chem. Phys.* **28,** 107 (1958).
76. McConnell, H. M., and Holm, C. H., *J. Chem. Phys.* **27,** 314 (1957).
77. McConnell, H. M., and Robertson, R. E., *J. Chem. Phys.* **29,** 1361 (1958).
78. McConnell, H. M., and Weaver, H. E., *J. Chem. Phys.* **25,** 307 (1956).
79. McLachlan, A. D., *Mol. Phys.* **3,** 233 (1960).
80. MacLean, C., and Mackor, E. L., *J. Chem. Phys.* **34,** 2207 (1961).
81. Maher, J. P., and Evans, D. F., *Proc. Chem. Soc.* p. 208 (1961).
82. Marshall, T. W., and Pople, J. A., *Mol. Phys.* **1,** 199 (1958).
83. Masuda, Y., *J. Phys. Soc. Japan* **11,** 670 (1956).
84. Meiboom, S., Loewenstein, A., and Alexander, S., *J. Chem. Phys.* **29,** 969 (1958).
85. Miller, H. C., unpublished results.
86. Moore, E. B., Jr., Dickerson, R. E., and Lipscomb, W. N., *J. Chem. Phys.* **27,** 209 (1957).
87. Muetterties, E. L., *J. Am. Chem. Soc.* **82,** 1082, 6429 (1960).
87a. Muetterties, E. L. "Advances in the Chemistry of the Coordination Compounds," p. 509. Macmillan, New York, 1961.
88. Muetterties, E. L., unpublished results.
88a. Muetterties, E. L., Bither, T. A., Farlow, M. W., and Coffman, D. D., *J. Inorg. & Nuclear Chem.* **16,** 52 (1960).
88b. Muetterties, E. L., and Phillips, W. D., *J. Am. Chem. Soc.* **79,** 322 (1957).
89. Muetterties, E. L., and Phillips, W. D., *J. Am. Chem. Soc.* **81,** 1084 (1959).
89a. Muller, N., Lauterbur, P. C., and Svatos, G. F., *J. Am. Chem. Soc.* **79,** 1043 (1957).
90. Muller, N., and Pritchard, D. E., *J. Chem. Phys.* **31,** 768 (1959).
91. Muller, N., and Pritchard, D. E., *J. Am. Chem. Soc.* **82,** 248 (1960).
92. Murray, G. R., and Waugh, J. S., *Ann. N. Y. Acad. Sci.* **70,** 900 (1958).
93. Myers, O. E., *J. Chem. Phys.* **28,** 1027 (1958).
94. Nordlander, J. E., and Roberts, J. D., *J. Am. Chem. Soc.* **81,** 1769 (1959); **82,** 6427 (1960).
95. Nordlander, J. E., Young, W. G., and Roberts, J. D., *J. Am. Chem. Soc.* **83,** 494 (1961).
96. Ogg, R. A., Jr., *J. Chem. Phys.* **22,** 560 (1954).

97. Ogg, R. A., Jr., *Discussions Faraday Soc.* **18,** 215 (1954).
98. Ogg, R. A., Jr., and Ray, J. D., *Discussions Faraday Soc.* **19,** 239 (1955).
99. Orgel, L. E., private communication to W. D. Phillips.
100. Pake, G. E., *J. Chem. Phys.* **16,** 327 (1948).
101. Phillips, W. D., unpublished results.
102. Phillips, W. D., *Ann. N. Y. Acad. Sci.* **70,** 817 (1958).
103. Phillips, W. D., and Benson, R. E., *J. Chem. Phys.* **33,** 607 (1960).
104. Phillips, W. D., Miller, H. C., and Muetterties, E. L., *J. Am. Chem. Soc.* **81,** 4496 (1959).
105. Pople, J. A., *Mol. Phys.* **1,** 3 (1958).
106. Pople, J. A., *Mol. Phys.* **1,** 168 (1958).
107 Pople, J. A., *J. Chem. Phys.* **24,** 1111 (1956).
108. Pople, J. A., Schneider, W. G., and Bernstein, H. J., "High Resolution Nuclear Magnetic Resonance." McGraw-Hill, New York, 1959.
109. Reference 108, Chapter VI.
110. Reference 108, Chapter XIII.
111. Reference 108, page 223.
112. Purcell, E. M., Torrey, H. C., and Pound, R. V., *Phys. Rev.* **69,** 37 (1946).
113. Ramsey, N. F., *Phys. Rev.* **78,** 699 (1950).
114. Ramsey, N. F., *Phys. Rev.* **91,** 303 (1953).
115. Ramsey, N. F., and Purcell, E. M., *Phys. Rev.* **85,** 143 (1952).
116. Reif, F., *Phys. Rev.* **100,** 1597 (1955).
117. Richards, R. E., and Smith, J. A. S., *Trans. Faraday Soc.* **47,** 1261 (1951).
117a. Rigden, J. S., Hopkins, R. C., and Baldeschwieler, E. L., *J. Chem. Phys.* **35,** 1532 (1961).
118. Rivkind, A. I., *Doklady Akad. Nauk S.S.S.R.* **102,** 1107 (1955).
119. Roberts, J. D., "Introduction to the Analysis of Spin-Spin Splitting in High Resolution Nuclear Magnetic Resonance Spectra," W. A. Benjamin, New York, 1961.
120. Roberts, J. D., "Nuclear Magnetic Resonance." McGraw-Hill, New York, 1959.
121. Sack, R. A., *Mol. Phys.* **1,** 163 (1958).
122. Saika, A., and Slichter, C. P., *J. Chem. Phys.* **22,** 26 (1954).
123. Schmutzler, R., Mahler, W., and Muetterties, E. L., unpublished results.
124. Shapiro, I., Williams, R. E., and Gibbins, S. G., *J. Phys. Chem.* **65,** 1061 (1961).
125. Shulman, R. G., *J. Chem. Phys.* **29,** 945 (1958).
126. Shulman, R. G., and Jaccarino, V., *Phys. Rev.* **108,** 1219 (1957).
127. Silver, A. H., and Bray, P. J., *J. Chem. Phys.* **29,** 984 (1958).
128. Smidt, J., and Hafner, W., *Angew. Chem.* **71,** 284 (1959).
129. Stranks, D. R., "Modern Coordination Chemistry" (J. Lewis and R. G. Wilkins, eds.), p. 95. Interscience, New York, 1960.
130. Tinkham, M. M., *Proc. Roy. Soc.* **A236,** 535 (1956).
131. Townes, C. H., and Dailey, B. P., *J. Chem. Phys.* **17,** 782 (1949).
132. Townes, C. H., and Dailey, B. P., *J. Chem. Phys.* **20,** 35 (1952).
133. Townes, C. H., Herring, C., and Knight, W. D., *Phys. Rev.* **77,** 852 (1950).
134. Tuttle, T. R., and Weissman, S. I., *J. Am. Chem. Soc.* **80,** 5342 (1958).
135. Van Vleck, J. H., *Phys. Rev.* **74,** 1168 (1948).
136. Waugh, J. S., and Fessenden, R. W., *J. Am. Chem. Soc.* **79,** 846 (1957).
137. Waugh, J. S., Humphrey, F. B., and Yost, D. M., *J. Phys. Chem.* **57,** 486 (1953).
138. Williams, R. E., Gibbins, S. G., and Shapiro, I., *J. Am. Chem. Soc.* **81,** 6164 (1959).
139. Wilkinson, G., *Proc. Chem. Soc.* p. 72 (1961).